② LEVEL II

NAVAL POSTGRADUATE SCHOOL
Monterey, California

DTIC
ELECTE
SEP 2 8 1981
S D
B

THESIS

RELATIONSHIPS BETWEEN SYNOPTIC STORM ACTIVITY
AND SEA SURFACE TEMPERATURE ANOMALIES OVER
THE NORTH PACIFIC OCEAN.

by

Bauke H. Houtman

June 1981

Thesis Advisor: Robert L. Haney

Approved for public release; distribution unlimited.

REPORT DOCUMENTATION PAGE		READ INSTRUCTIONS BEFORE COMPLETING FORM
1. REPORT NUMBER	2. GOVT ACCESSION NO. $A104\,590$	3. RECIPIENT'S CATALOG NUMBER
4. TITLE (and Subtitle) Relationships between Synoptic Storm Activity and Sea Surface Temperature Anomalies over the North Pacific Ocean		5. TYPE OF REPORT & PERIOD COVERED Master's Thesis; June 1981
		6. PERFORMING ORG. REPORT NUMBER
7. AUTHOR(s) Bauke H. Houtman		8. CONTRACT OR GRANT NUMBER(s)
9. PERFORMING ORGANIZATION NAME AND ADDRESS Naval Postgraduate School Monterey, California 93940		10. PROGRAM ELEMENT, PROJECT, TASK AREA & WORK UNIT NUMBERS
11. CONTROLLING OFFICE NAME AND ADDRESS Naval Postgraduate School Monterey, California 93940		12. REPORT DATE June 1981
		13. NUMBER OF PAGES 82
14. MONITORING AGENCY NAME & ADDRESS(if different from Controlling Office)		15. SECURITY CLASS. (of this report) Unclassified
		15a. DECLASSIFICATION/DOWNGRADING SCHEDULE

16. DISTRIBUTION STATEMENT (of this Report)

Approved for public release; distribution unlimited.

17. DISTRIBUTION STATEMENT (of the abstract entered in Block 20, if different from Report)

18. SUPPLEMENTARY NOTES

19. KEY WORDS (Continue on reverse side if necessary and identify by block number)

Air-sea interaction
Anomalous storminess
Sea-surface temperature anomalies

20. ABSTRACT (Continue on reverse side if necessary and identify by block number)

The significance of year-round relationships between synoptic storm activity and sea-surface temperature (SST) over the North Pacific Ocean for the period January 1969 through December 1978, were examined using cross-correlation analysis. The possible existence of a seasonal dependence in the SST-wind relationships was examined using sub-sample record cross-correlation analysis and model tests with both a constant and a variable mixed-layer depth, respectively. Wind forcing data was represented by ($U*^3$), friction velocity cubed, and wind stress curl ($CURL_z\tau$),

DD FORM 1473 EDITION OF 1 NOV 68 IS OBSOLETE
1 JAN 73
(Page 1)   S/N 0102-014-6601

as computed from: (a) High-pass filtered wind components only (periods less than ten days), (b) High- and Low-pass filtered wind components which includes the interaction terms and (c) the unfiltered (total) wind components.

The correlation maps of SST with both $(U_*^3)H$ and $(U_*^3)HL$, calculated from the ten-year record, showed large areas of significant negative values in the midlatitude North Pacific Ocean when the SST was lagged by any amount from zero- to three-months. Lag correlations involving (U_*^3) from (c) and $(CURL_z\tau)$ were considerably less significant. Zero lag correlations between $\partial/\partial t$ SST and the various wind parameters generally substantiated the above results except for revealing a large and significant positive correlation between $\partial/\partial t$ SST and the $(CURL_z\tau)$ (from (c)) off the West Coast of North America.

The sub-sample record examination resulted in generally low significance levels and no statistical confidence as to the existence of a seasonal variation in the relationships. Model tests involving a prescribed, seasonally varying, mixed-layer depth showed that there was no detectable seasonal variation in the SST-wind relationships.

Accession For	
NTIS GRA&I	✓
DTIC TAB	☐
Unannounced	☐
Justification	
By	
Distribution/	
Availability Codes	
Dist	Avail and/or Special
A	

Relationships between Synoptic Storm Activity
and Sea Surface Temperature Anomalies over
the North Pacific Ocean

by

Bauke H. Houtman
Lieutenant, United States Navy
B.S., University of California at Los Angeles, 1975

Submitted in partial fulfillment of the
requirements for the degree of

MASTER OF SCIENCE IN METEOROLOGY AND OCEANOGRAPHY

from the

NAVAL POSTGRADUATE SCHOOL
June 1981

Author _____

Approved by: _____
Thesis Advisor

_____
Second Reader

_____
Chairman, Department of Meteorology

_____
Dean of Science and Engineering

3

ABSTRACT

The significance of year-round relationships between synoptic storm activity and sea-surface temperature (SST) over the North Pacific Ocean for the period January 1969 through December 1978, were examined using cross-correlation analysis. The possible existence of a seasonal dependence in the SST-wind relationships was examined using sub-sample record cross-correlation analysis and model tests with both a constant and a variable mixed-layer depth, respectively. Wind forcing data was represented by $(U_\star^3)$, friction velocity cubed, and wind stress curl $(CURL_Z\tau)$, as computed from: (a) High-pass filtered wind components only (periods less than ten days), (b) High- and Low-pass filtered wind components which includes the interaction terms and (c) the unfiltered (total) wind components..

The correlation maps of SST with both $(U_\star^3)H$ and $(U_\star^3)HL$, calculated from the ten-year record, showed large areas of significant negative values in the midlatitude North Pacific Ocean when the SST was lagged by any amount from zero- to three-months. Lag correlations involving $(U_\star^3)$ from (c) and $(CURL_Z\tau)$ were considerably less significant. Zero lag correlations between $\partial/\partial t$ SST and the various wind parameters generally substantiated the above results except for revealing a large and significant _positive_ correlation between $\partial/\partial t$ SST and the $(CURL_Z\tau)$ (from (c)) off the West Coast of North America.

The sub-sample record examination resulted in generally low significance levels and no statistical confidence as to the existence of a seasonal variation in the relationships. Model tests involving a prescribed, seasonally varying, mixed-layer depth showed that there was no detectable seasonal variation in the SST-wind relationships.

TABLE OF CONTENTS

LIST OF FIGURES

7

8

ACKNOWLEDGEMENTS

I. INTRODUCTION

This study examined the relationships between synoptic storm activity and sea-surface temperature (SST) over the North Pacific Ocean from 20° N to 60° N and 110° W to 130° E for the period January 1969 to December 1978. The hypothesis tested is that the monthly mean sea surface temperature responds to atmospheric wind forcing, as manifested in storms, and that the amount of response is proportional to the amount of wind forcing. The concept for examining storminess comes from the strong relationship that exists between synoptic storms and air-sea exchange (Simpson (1969), Fissel, Pond and Miyake (1977), Elsberry and Camp (1978)) and previous work accomplished in this area by Little (1980).

The major goal of the study was to obtain a quantitative measure of the statistical significance of the year-round relationships between SST and wind forcing found by Little (1980). This was done using the method of Sciremammano (1979) and the results are shown in Section III. A second major goal of this study was to investigate the possible existence of seasonal dependence in the SST-wind relationships. This was done using two different methods and these results are shown in Section IV. A third objective of this study was to examine how well the SST-surface wind relationships can be seen using conventional data on storm tracks and storm frequencies. The results of this examination are shown in Section IV.

The approach and expectations of this study were that: 1) Application of the method of Sciremammano (1979), for the determination and

11

presentation of statistical significance between two time series of geo-physical data, would produce a quantitative measure of the significance of the year-round relationships between SST and the chosen wind forcing parameters, friction velocity and wind stress curl. It was expected that significant negative correlations would occur when the SST lagged the wind parameters, in support of the hypothesis that anomalous stormi-ness leads to subsequent ocean surface cooling. 2) Examination into the seasonal dependence of relationships between SST, $\partial/\partial t$ SST, and the wind parameters would, perhaps, reveal stronger correlations and greater significance during the summer months when the mixed layer is shallowest and weaker correlations and less significance during the winter months when the mixed layer is deepest. 3) Further insight into the dynamics of the relationships between SST, $\partial/\partial t$ SST, and the wind parameters could be obtained by examination of a particular month or series of months in the ten-year record when the correlations were especially significant.

The data sets used in this study were obtained from Little (1980). The atmospheric data were prepared by Fleet Numerical Oceanography Center (FNOC) from a special ten-year series of six-hourly surface wind analyses. Friction velocity cubed (U_*^3) and the vertical component of the curl of the wind stress ($CURL_z\tau$) were calculated from the wind data. These para-meters were chosen because of the direct relationship between (U_*^3) and mechanical mixing of the sea by the overlying atmosphere and the well-established relationship between the wind stress curl and Ekman conver-gence and divergence. Six-hourly values of both (U_*^3) and curl were com-puted using a) High-pass filtered wind components only (periods of less

12

than ten days), b) a combination of High- and Low-pass filtered wind
components which includes the interaction terms, and c) the unfiltered
(total) wind components. Monthly means, long term (10 years) monthly
means, and monthly anomalies of each of the six wind parameters were
calculated for comparison with monthly SST anomalies. The six wind
parameter and SST anomaly fields were truncated to reduce "noise"
using Empirical Orthogonal Function (EOF) analysis. Normalized cross
correlations of the resulting seven data sets were utilized to examine
the relationships between monthly anomalies of SST and synoptic storm
activity, as represented by the wind parameters.

II. DATA SET DESCRIPTION

This section describes the origin and preliminary processing that was done to the data sets used in this study.

A. SEA SURFACE TEMPERATURE

A ten-year time series of monthly sea-surface temperature (SST) data, covering the period January 1969 through December 1978, had been previously obtained from Scripps Institution of Oceanography Climate Research Group through the generosity of Jerome Namias and Robert Born (Little (1980)). The data are geographically located at 166 grid points (equally spaced at 5° latitude-longitude intervals) in the North Pacific Ocean, covering the area from 20° N to 60° N and 110° W to 130° E (see Figure 1 Little (1980)). Each monthly temperature value was converted from Fahrenheit to Centigrade and processed to compute the anomaly by finding the difference between the monthly value and the ten-year average for the same grid point and month of year. A 120-month record of SST anomalies at each of the 166 grid points was thus constructed.

B. FRICTION VELOCITY AND SURFACE STRESS

Monthly anomalies of six different surface wind parameters involving the cube of the friction velocity (U_*^3), and the curl of the surface stress, ($CURL_z\tau$), had been previously obtained from Haney, Risch and Heise (1981) by Little (1980). All six wind parameters were calculated from six-hourly surface wind analyses over the North Pacific Ocean

14

prepared by Fleet Numerical Oceanography Center (FNOC) for the same ten year period, January 1969 through December 1978. The six wind parameters were calculated as follows.

Synoptic storm activity having time scales less than ten days was extracted from the time series of surface wind at each grid point by the use of a symmetric high pass Gaussian filter. The wind parameters (U_*^3 and $CURL_z\tau$) were then calculated from a) the High-pass filtered wind components only, b) a combination of High- and Low-pass filtered wind components, and c) the total unfiltered wind components, respectively. Monthly means, long term (10 years) monthly means and finally monthly anomalies of each wind parameter were constructed and interpolated from the FNOC Polar Stereographic Grid to the 166 point SST grid.

Little (1980) accomplished further analysis. All seven anomaly data sets (the SST and the six wind parameters) were detrended and standardized to remove linear trends in the anomalies. Empirical Orthogonal Function (EOF) analysis was then performed on all seven data sets in an effort to enhance the "signal" by reducing the "noise" using the technique of Preisendorfer and Barnett (1977). A varying number of EOF modes were retained for each of the data sets resulting in the final seven data sets being truncated, or filtered versions of the original data sets. The amount of total variance retained in the data sets was of the order of 62 to 76 percent (see Little (1980)).

Possible relationships between the data sets are examined in the following sections. Section III examines the relationships that exist year-round between SST and each of the six wind parameters. Based upon

15

the results of that analysis, Section IV narrows the field of interest down to SST, $\partial/\partial t$ SST and (U_*^3) calculated from the combination of High- and Low-pass filtered winds, and investigates the possibility of seasonal dependence in the relationships. Finally, in Section IV, the sequence September, October, November 1977 is examined in an effort to gain further insight into the dynamics of the relationships between SST and (U_*^3)HL.

III.   YEAR ROUND RELATIONSHIPS BETWEEN WIND AND SST

A.   CALCULATIONS PERFORMED

1.   Raw Correlations

In order to investigate relationships between the wind and SST, raw correlation values were determined between SST and each of the six atmospheric forcing functions. The complete data records of 120 months were utilized to calculate cross correlations between SST and each of the wind parameters at lags of minus three-to plus five-months. A lag of minus three-months means the wind parameter is correlated with the SST which occurred three months previous, whereas a plus three-month lag means the wind parameter is correlated with SST occurring three months later. Of interest in this study is atmospheric forcing of the ocean and thus emphasis is placed on evaluating the positive lags.

Correlation values were computed over the entire grid and contoured at intervals of 0.1. Spatial maps of the raw correlations for minus three-to plus three-month lags are presented in Little (1980) and for this reason have been omitted here. The conclusions by Little (1980) were that there is apparently significant negative correlation between the SST and wind forcing based on the (approximate) significance level criteria used in his study.

2.   Significance Levels

Interpretation of the raw correlations eventually requires some consideration of the significance levels. Little (1980) made use of a

17

critical correlation value derived from Davis (1976) in which a correlation, r, was considered significantly different from zero if $|r| >$ 0.20. The critical correlation value of 0.20 was determined by a qualitative estimate of the number of independent events in the records. It was also suggested by Little (1980) that perhaps a quantitative estimate of the critical value could be obtained by the use of the technique presented by Sciremammano (1979). Sciremammano (1979) derived a convenient method for determining and presenting significance levels of cross correlations which is equivalent to that of Davis (1976). This approach normalizes the raw correlations by a large lag standard error, σ, which is estimated by the Bartlett formula

$$\sigma^2 = \frac{1}{N} \sum_{i=-\infty}^{i=+\infty} CX(i) \; CY(i) \tag{1}$$

Here $CX(i)$ and $CY(i)$ are the discrete autocorrelation functions of the input processes, $X(i) = X(i\Delta t)$, $Y(i) = Y(i\Delta t)$ and N is the number of discrete observations.

The value of σ estimates the artificial correlation between the two parameters which arises from the interplay of the dominant time scales of the input processes (represented by the summation of $CX(i)CY(i)$ in (1)) and the record length N. Normalization of the raw correlations by σ immediately shows the significance of the correlations since, to a good approximation, $C99 \approx 2.6 \; \sigma$, $C95 = 2.0 \; \sigma$, and $C90 = 1.7 \; \sigma$ for a time series involving at least 10 degrees of freedom. As shown by Sciremammano (1979), this requirement is fulfilled when $n \equiv \frac{1}{\sigma^2} \geq 10$.

18

For lagged correlations the equation is modified somewhat and becomes

$$\sigma_K^2 = \frac{1}{N-K} \sum_{i=-\infty}^{i=+\infty} CX(i)\ CY(i) \tag{2}$$

where K is the magnitude of the lag (K>0) and N-K is the effective record length. Thus the only difference between the value of σ given by (1) and (2) is due to the slightly shorter record that is necessary when calculating lagged correlations. This dependence on the effective record length is not very strong since σ_K is inversely proportional to the square root of N-K, and usually N>>K.

Application of this normalization procedure to the raw correlations requires a practical evaluation of the summation shown in (2). This was done by writing

$$\hat{\tau} = \sum_{-I}^{+I} CX(i)\ CY(i) \tag{3}$$

where $\hat{\tau}$ is a bivariate integral time scale (expressed nondimensionally in units of Δt), and I is the maximum value of the summation index i. Enfield and Allen (1980) suggest the summation limit I be determined such that successive values of $\hat{\tau}$, obtained by increasing I, change very little. For this study, the autocorrelation functions were computed for all i in the range -23<i<23. The summation limit, I, in (3) was determined such that successive values of $\hat{\tau}$ changed less than 1%. This criteria was met in all six pairs of cross correlations (between SST and

19

each wind parameter) for I<14. The resulting σ values for all lags were on the order of 0.1 over the entire grid.

Figure 1 shows a plot of two typical autocorrelation functions at a particular grid point in the Mid-North Pacific Ocean. It is seen that the time scales of the SST events are on the order of eight or nine months, whereas those of the (U_*^3)HL events are typically two to four months. Figure 2 shows the value of σ calculated for these variables over the entire grid.

The raw lagged correlations (between SST and a given wind parameter) at each grid point were normalized by the (appropriate) σ_K value for that grid point, yielding normalized lagged correlations on the order of one to three. The results are presented below. As noted above, a value of 2 is significant at the 95 percent confidence level while a value of 3 is significant at the 99 percent level.

B. RESULTS

1. Lag Correlations between (U_*^3) and SST

Figures 3 to 11 are maps of normalized correlations between the three (U_*^3) wind parameters and SST for minus three-to plus five-month lags. Positive lags are for SST lagging the wind. Figures 3 to 5 contain the correlations between SST and (U_*^3)H computed from the High-pass wind components only, Figures 6 to 8 contain the correlations between SST and (U_*^3)HL computed from a combination of High- and Low-pass wind components and Figures 9 to 11 contain the correlations between SST and (U_*^3)TOT computed from the unfiltered (total) wind components. In each map, shaded areas are indicative of negative correlations and the contour interval is 1.0.

20
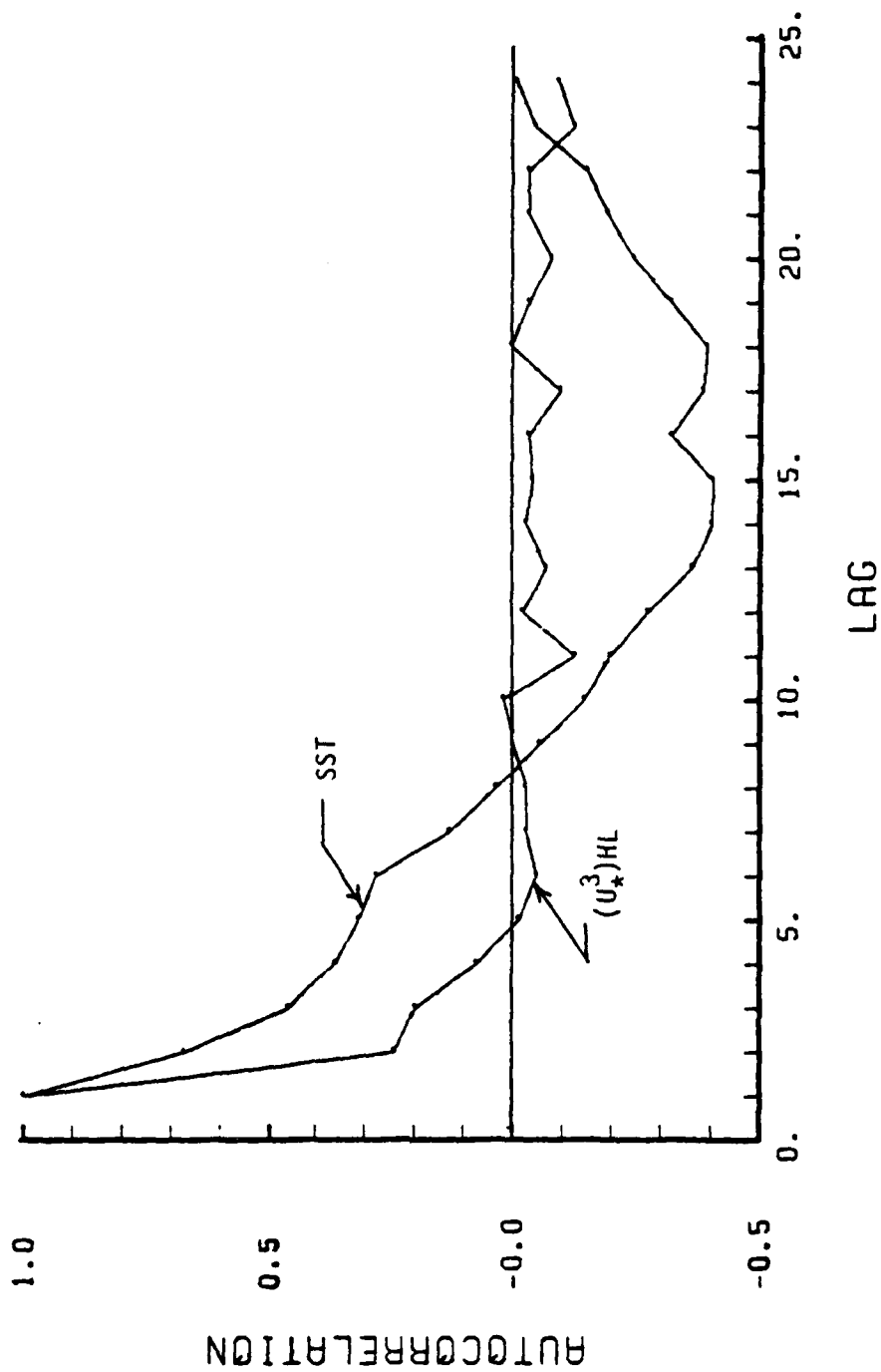
Figure 1. SST and $(U_\star^3)_{HL}$ autocorrelation functions vs lag. Positive lags only are shown since the functions are symmetric.

21
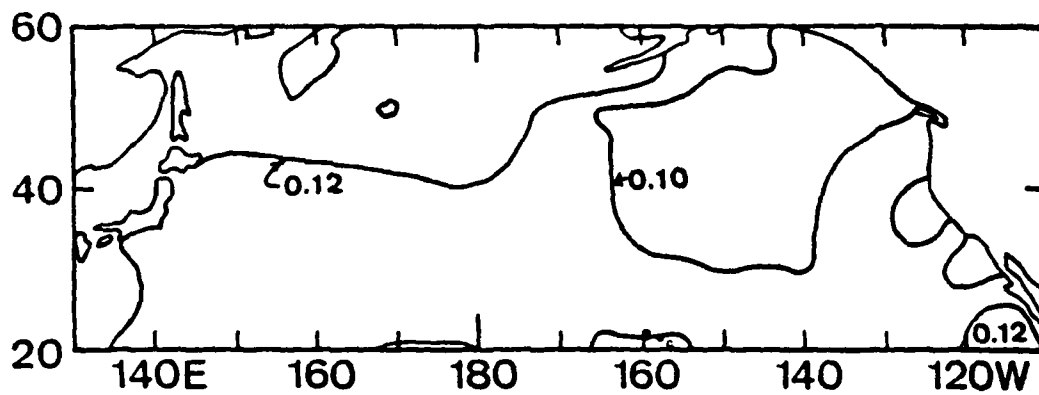
Figure 2. Zero lag σ values for the variables SST and $(U_*^3)HL$ based on a 120-month record. Contour interval is 0.02.

$(U_\star^3)H$

LAG = -3

LAG = -2

LAG = -1

140E   160   180   160   140   120W
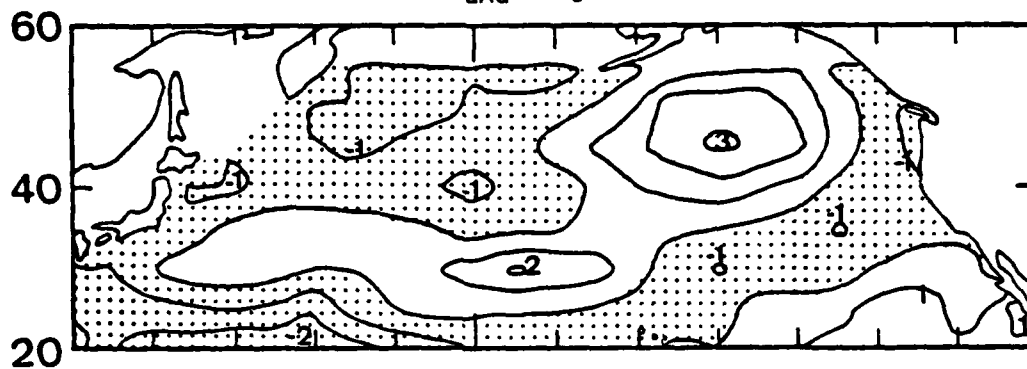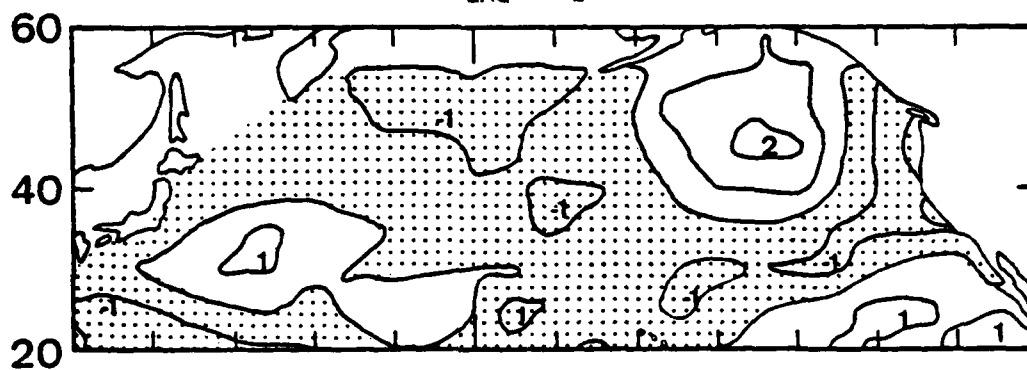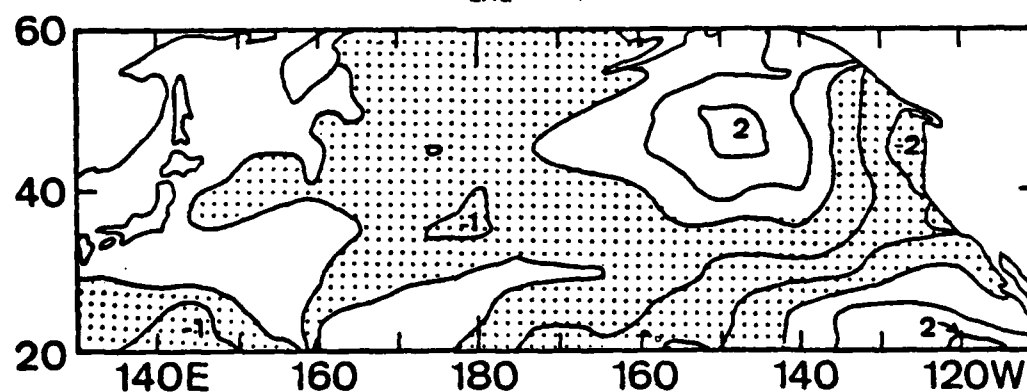
Figure 3. Normalized correlation between $(U_\star^3)H$ and SST at -3, -2, and
          -1 month lag. Contour interval is 1 and several closed
          contours are labeled. Shaded areas denote negative values.

23

$(U_*^3)H$
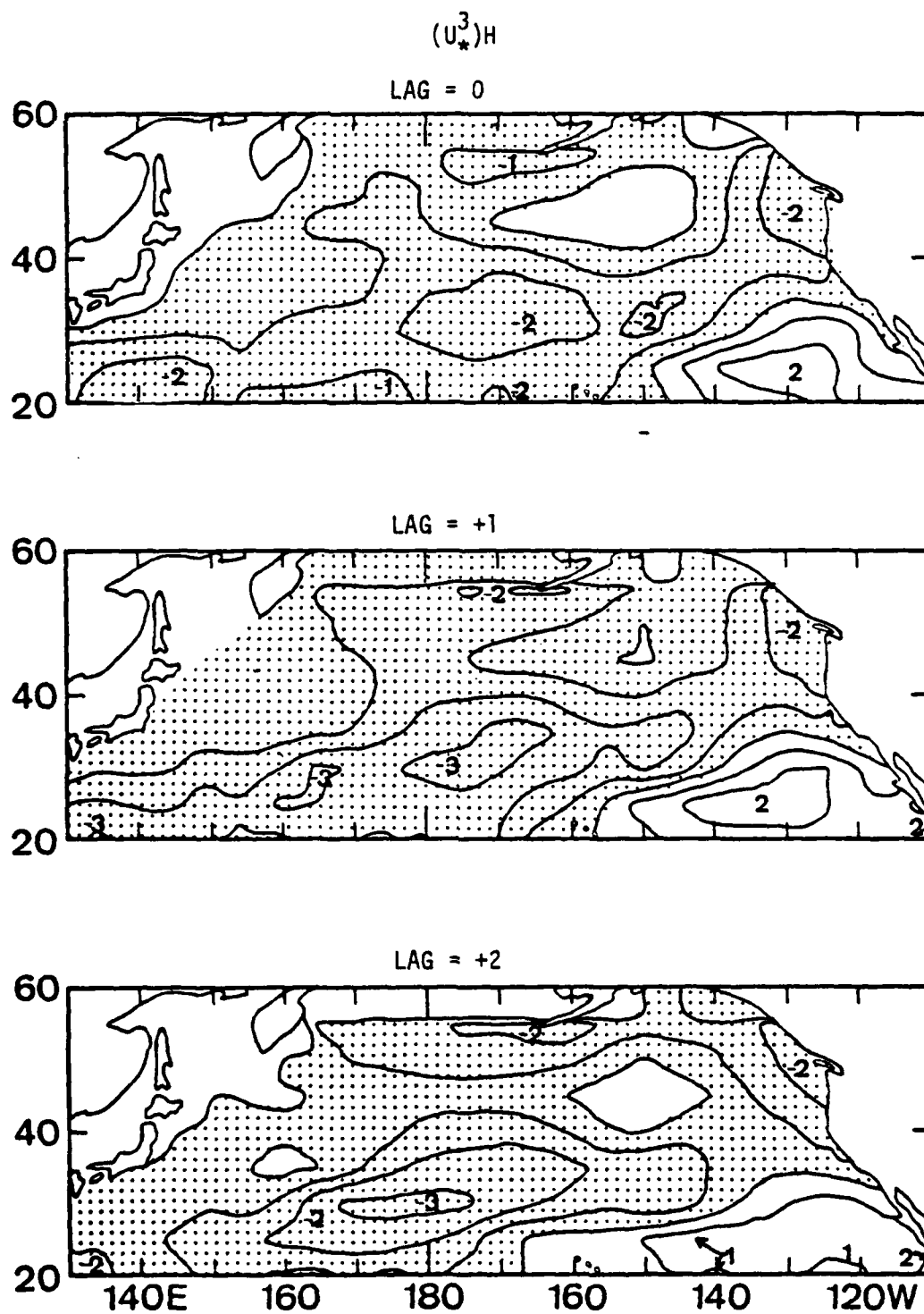
LAG = 0

LAG = +1

LAG = +2

Figure 4. Same as Fig. 3 except for 0, +1 and +2 month lags.

24

$$(U_*^3)H$$
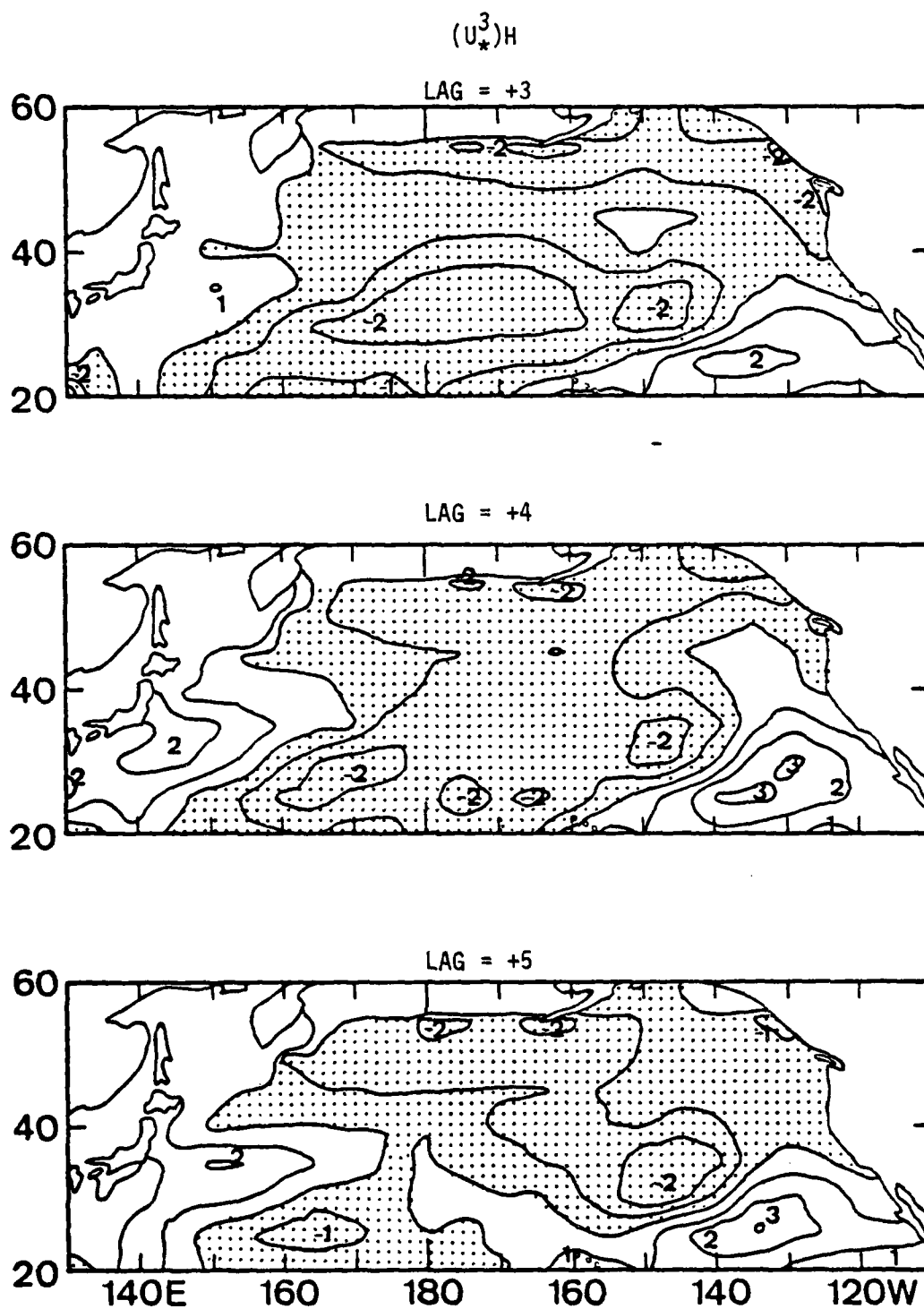
Figure 5. Same as Fig. 3 except for +3, +4 and +5 month lags.

25
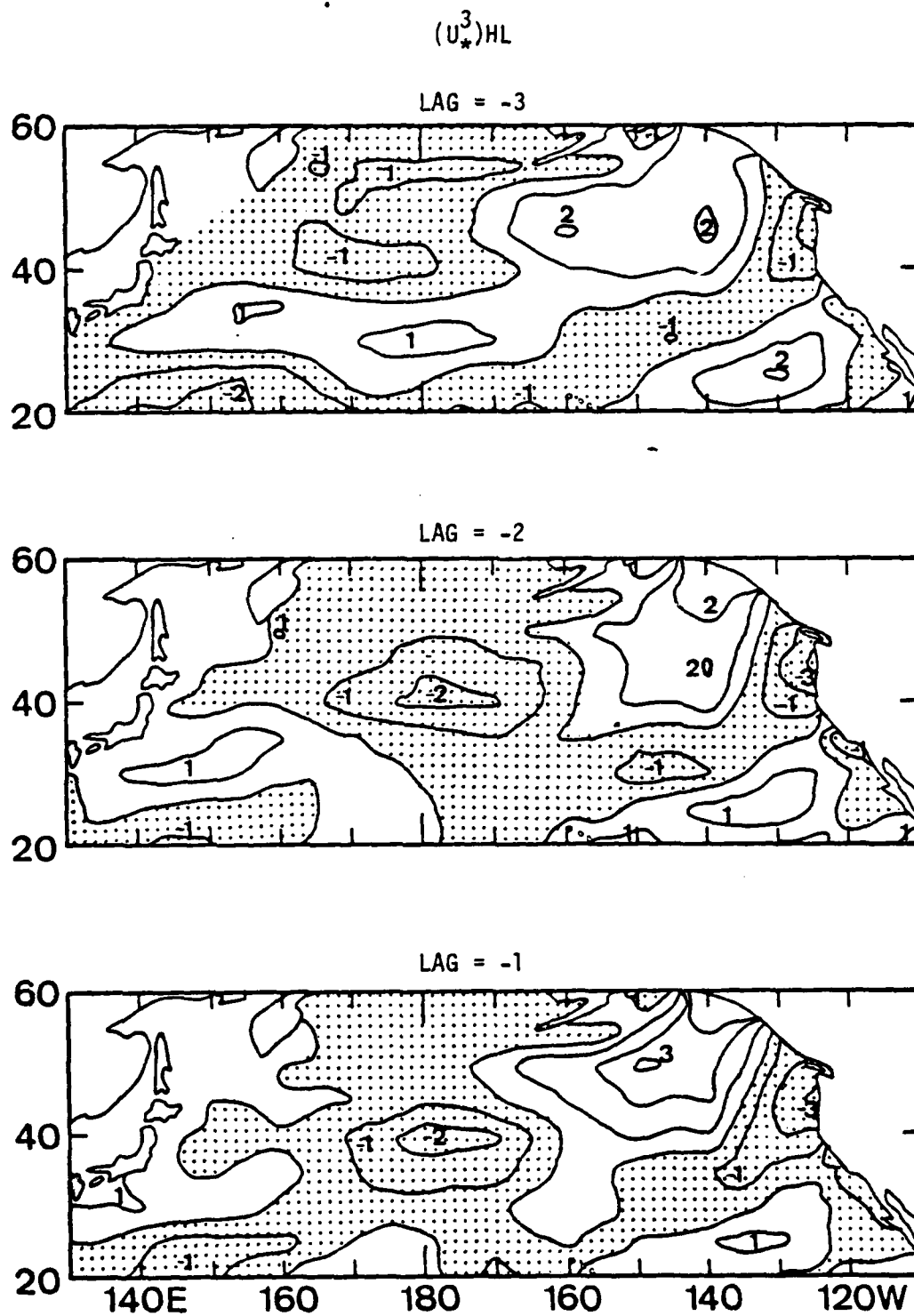
(U_*^3)HL

Figure 6. Same as Fig. 3 except for (U_*^3)HL.

26

$(U_*^3)HL$

LAG = 0

LAG = +1

LAG = +2

140E   160   180   160   140   120W
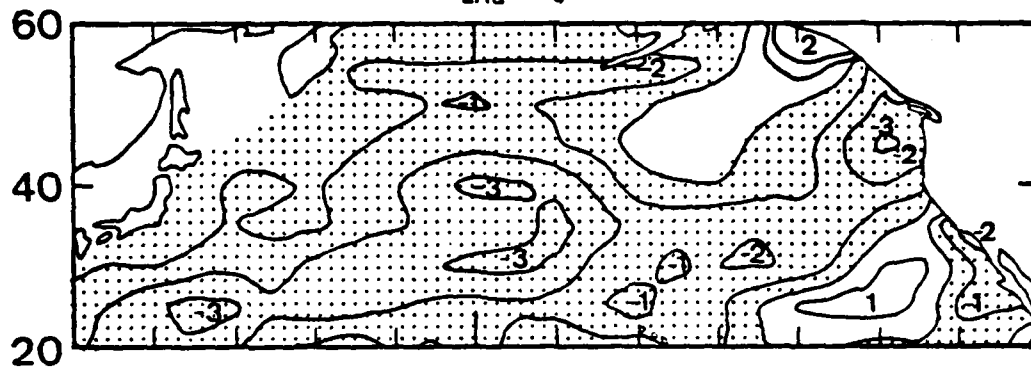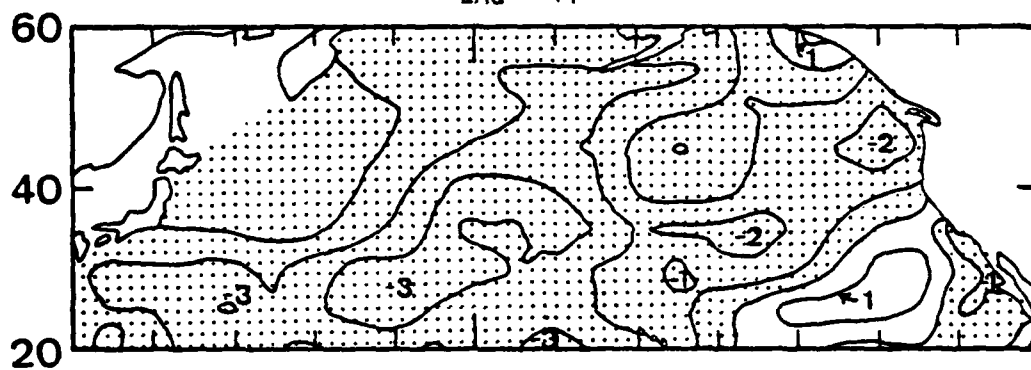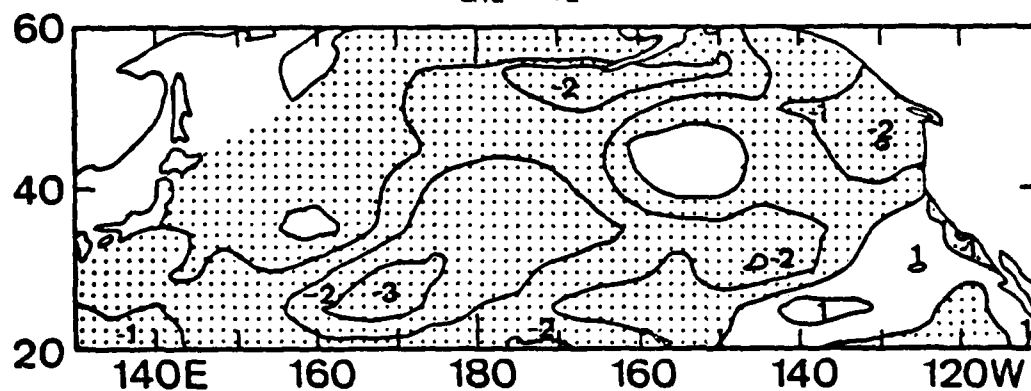
Figure 7.   Same as Fig. 6 except for 0, +1 and +2 month lags.

$(U_*^3)HL$
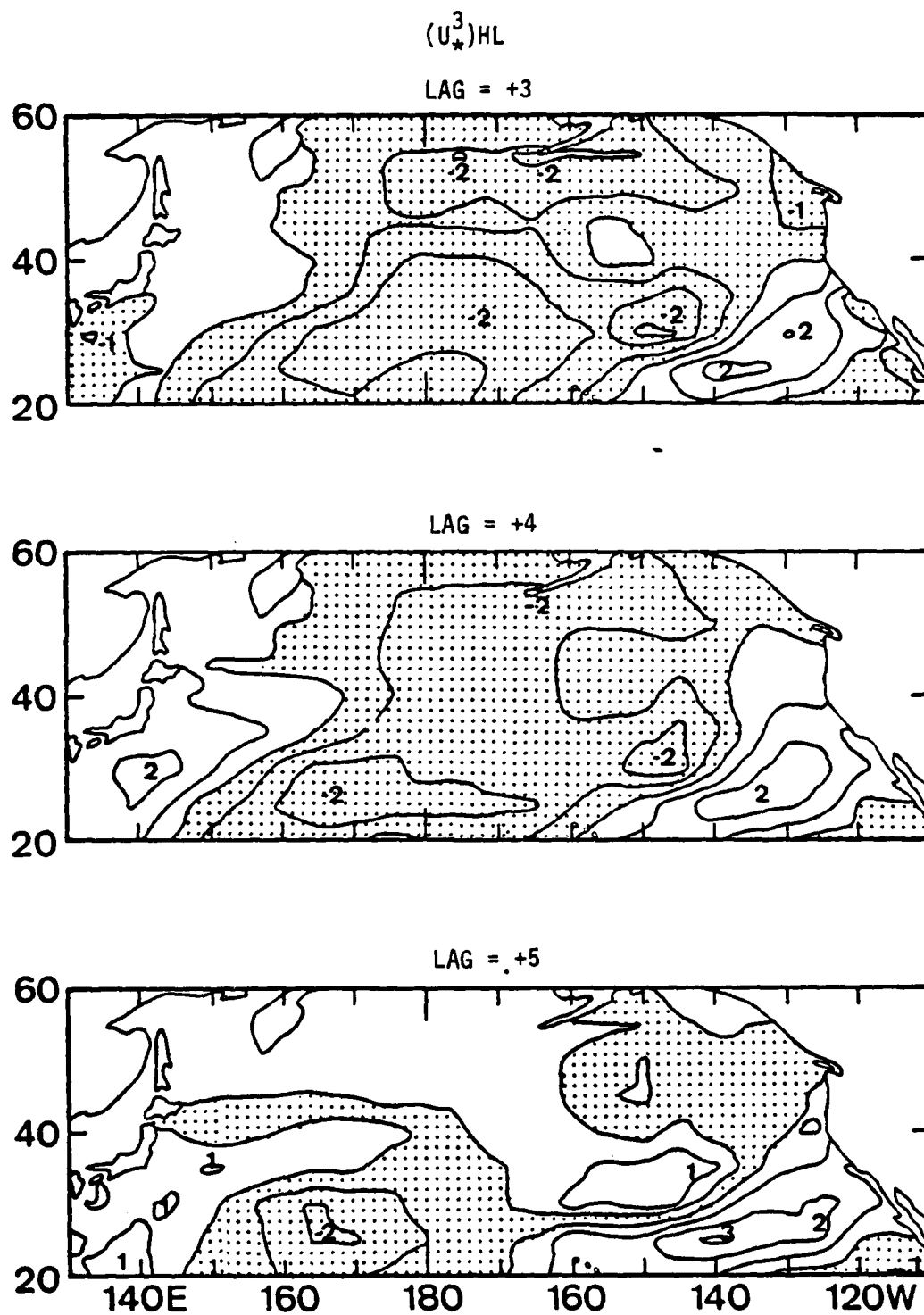
LAG = +3

LAG = +4

LAG = +5

Figure 8. Same as Fig. 6 except for +3, +4 and +5 month lags.

28
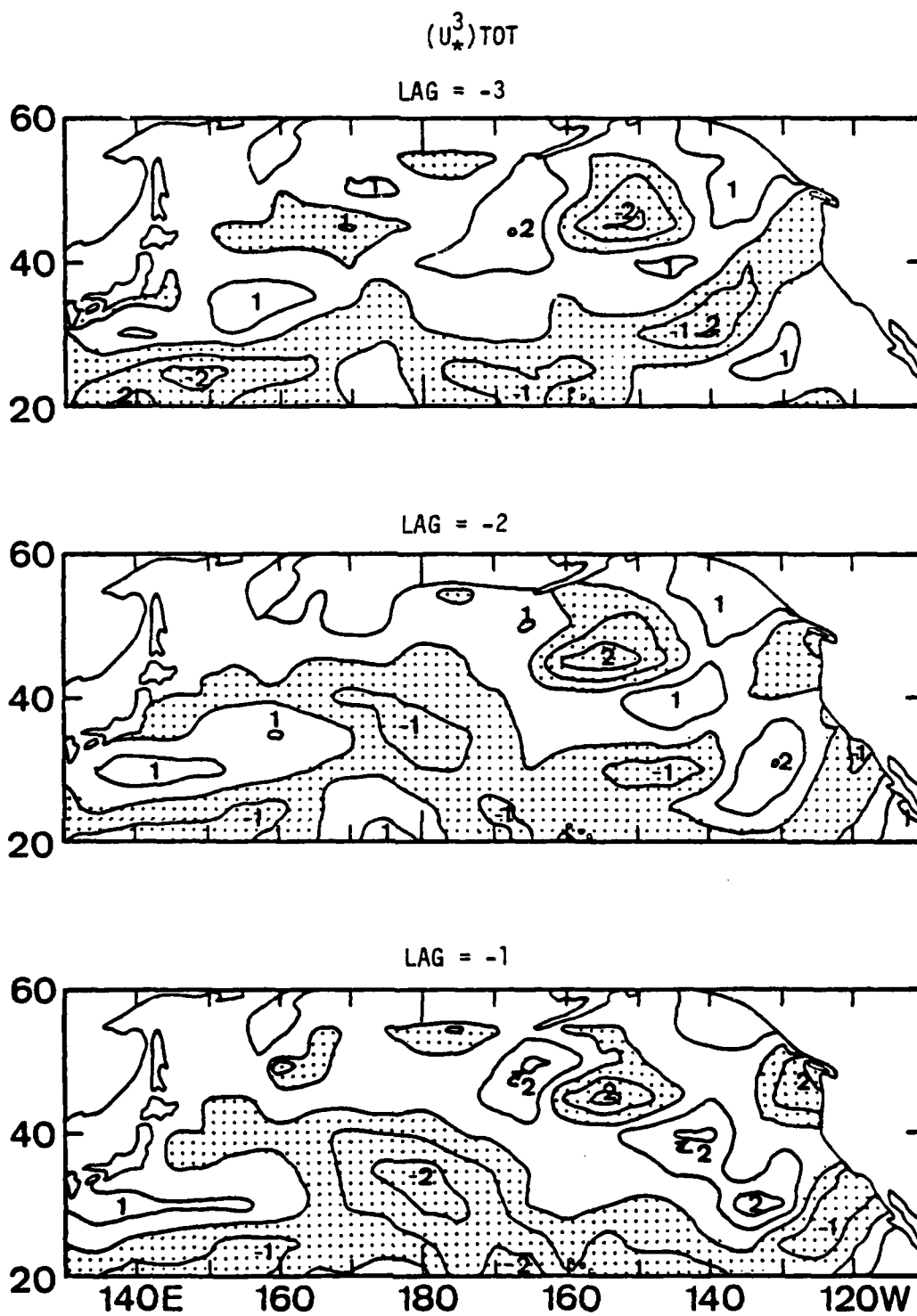
Figure 9. Same as Fig. 3 except for (U_*^3)TOT.
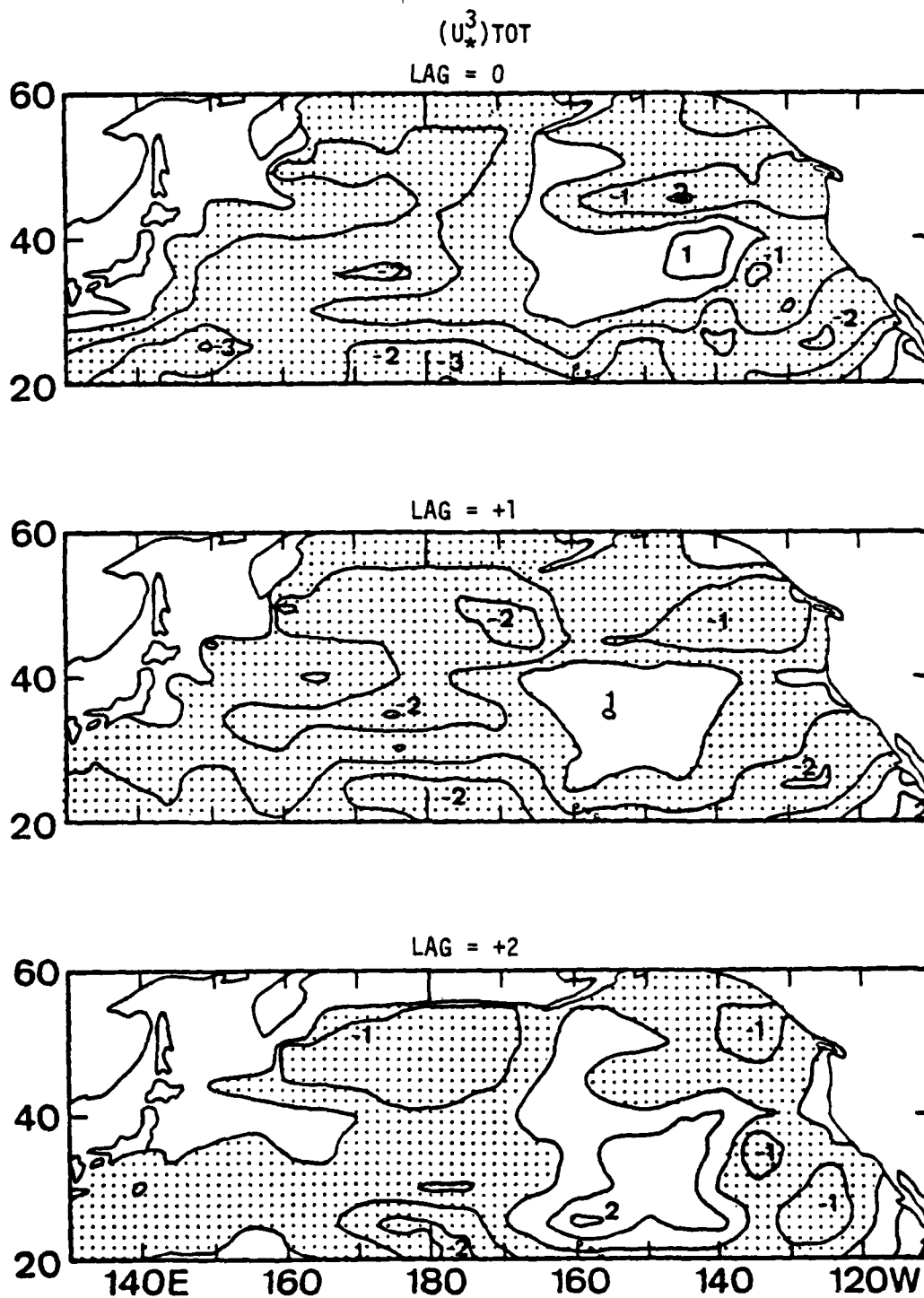
Figure 10. Same as Fig. 9 except for 0, +1 and +2 month lags.

$(U_*^3)_{TOT}$

LAG = +3
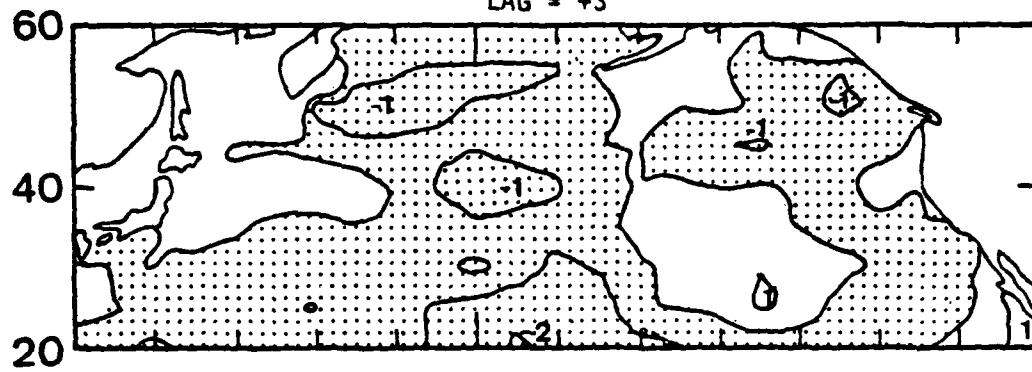
LAG = +4
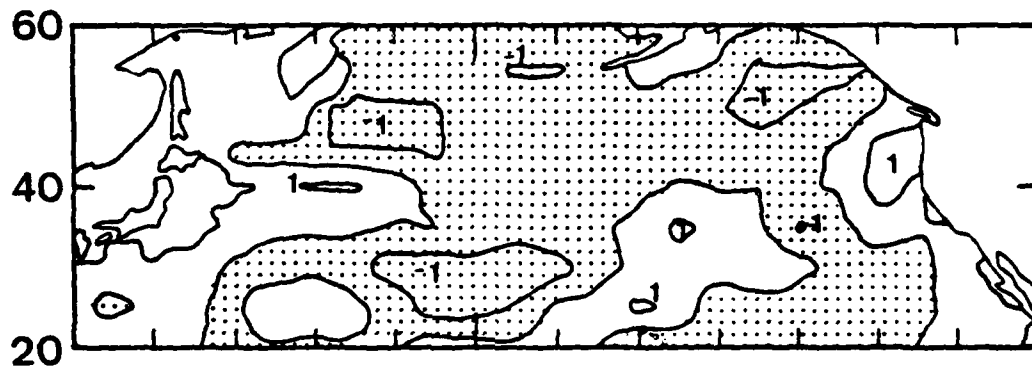
LAG = +5
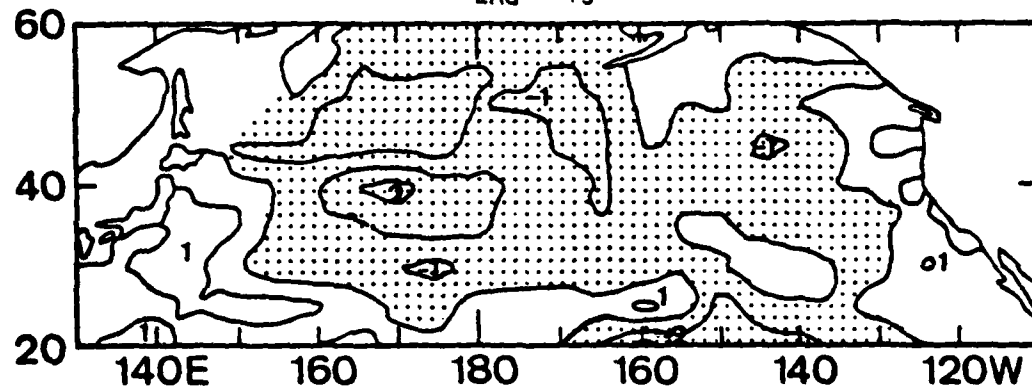
Figure 11.   Same as Fig. 9 except for +3, +4 and +5 month lags.

31

Examination of the map series reveals negative correlations over large areas of the grid for the zero and positive lags. This result is consistent with the hypothesis that anomalous surface wind forcing produces subsequent anomalous surface cooling. The significance levels of the correlations are also immediately seen, recalling C95 = 2.0 σ and C99 = 2.6 σ. Large areas with values of 2.0 and 3.0 are noted in Figures 3 to 11; however, only those areas which are clearly greater than 5% of the total grid area will be considered.

Figures 4 and 5 indicate a region of significant negative correlation in the Mid-North Pacific Ocean between $(U_*^3)H$ and SST for the zero-to plus three-month lags. The area is located at approximately 30° N 180° W trending northeast-southwest and consisting of normalized correlation values of 2.0 and 3.0. A similar geographic region of significant negative normalized correlations is seen in Figures 7 and 8 for $(U_*^3)HL$ and SST. Here also the region appears in the zero-to plus three-month lags. Other limited areas of magnitude 2.0 and 3.0 are present in (nearly) all the figures but are not considered of importance in this study due to their incoherent spatial distribution and/or the small percentage of total map area that they occupy. The presence of significant correlations of $(U_*^3)H$ and $(U_*^3)HL$ with SST indicates that over these areas of the North Pacific Ocean, above normal synoptic storm activity during a month occurs with and is followed by monthly values of below normal SST. This occurrence at lags of zero out to plus three-months appears to show that the ocean's response to anomalous storm activity is both immediate and long lasting.

32

A brief examination of the minus three-month to minus one-month lags for $(U_*^3)H$ and $(U_*^3)HL$ (Figures 3 and 6) indicates an area of significant positive correlation in the Gulf of Alaska region. This appears to show ocean forcing atmosphere, vice atmosphere forcing ocean, in that warmer than normal SST is correlated with subsequent above normal storminess (and cold SST with below normal storminess). This result will not be pursued further since the present study is primarily designed (through the particular choice of atmospheric parameters) to investigate the possible forcing of the ocean by the atmosphere.

2. Lag Correlations between $CURL_z\tau$ and SST

Normalized correlations between SST and the three wind stress curl parameters for lags of minus three-to plus five-months are presented in Figures 12 to 20. The format of the figures is similar to that for (U_*^3). SST is again lagged relative to curl with a lag of plus one-month showing the correlation between the curl field and the SST field which occurred one month later. The contour interval is 1.0 and negative correlation areas are shaded. Similar results of large areas of negative correlations were expected between the curl parameters and SST for zero and positive lags since anomalous values of wind stress curl indicate anomalous Ekman pumping.

Examination of the curl map series (Figures 12 to 20) immediately shows the existence of less spatial coherence for the curl than was seen for the friction velocity (Figures 3 to 11). This is especially true for the storm related curl parameters. In addition, although negative correlation areas are present at positive lag, they are less dominate and cover less total grid area than for the friction velocity. Areas of

33

$(CURL_Z\tau)H$

Figure 12. Same as Fig. 3 except for $(CURL_Z\tau)H$.

34

$(CURL_z\tau)H$
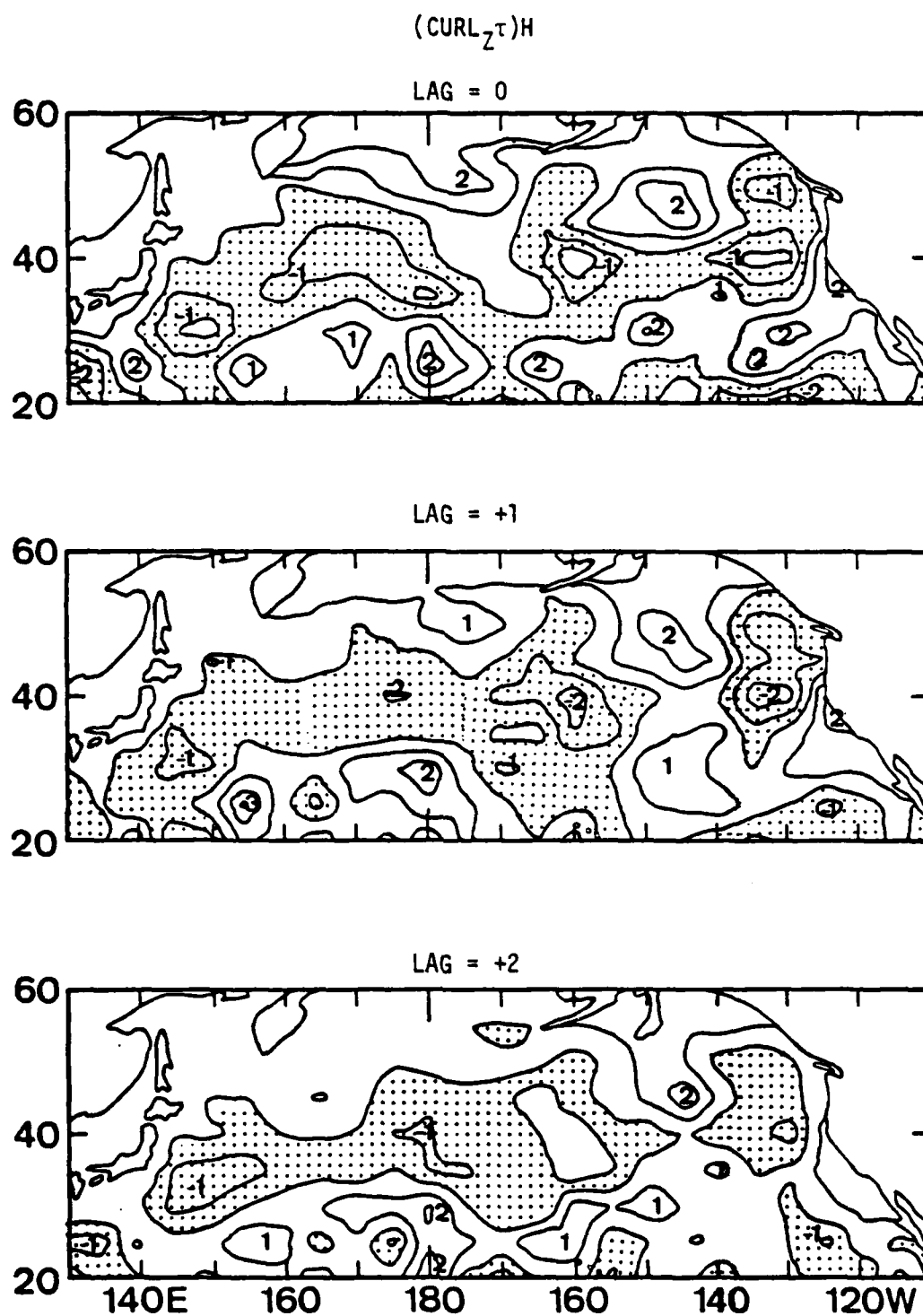
LAG = 0

LAG = +1

LAG = +2

Figure 13. Same as Fig. 12 except for 0, +1 and +2 month lags.

35

$(CURL_Z\tau)H$

LAG = +3

LAG = +4

LAG = +5
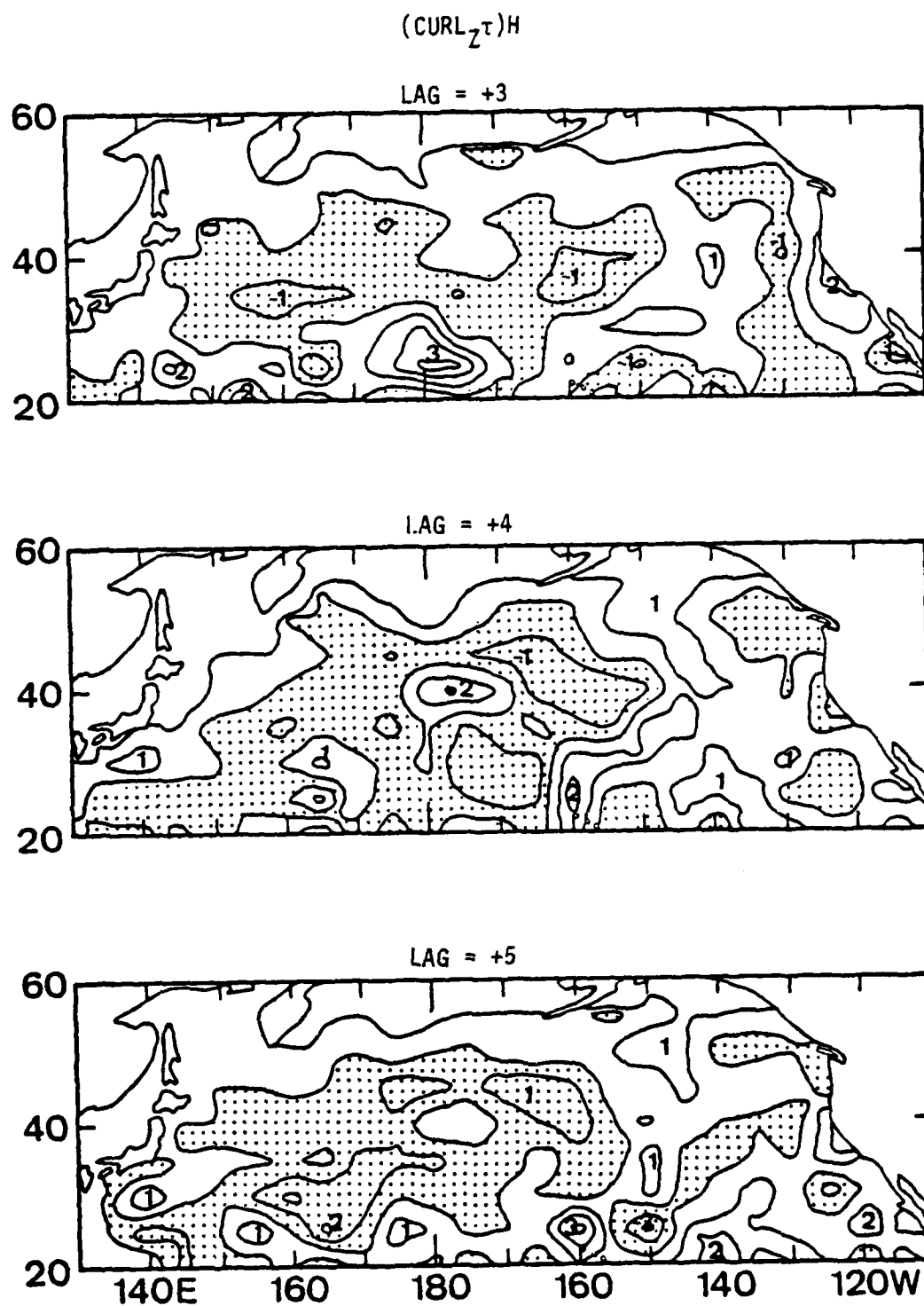
Figure 14. Same as Fig. 12 except for +3, +4 and +5 month lags.
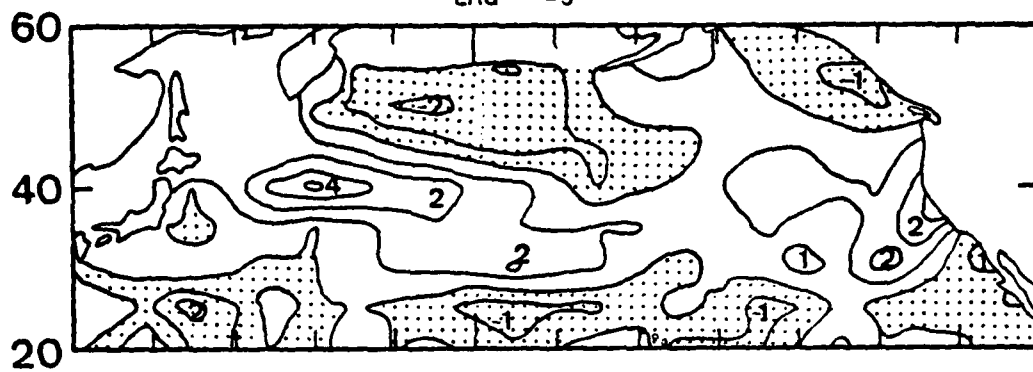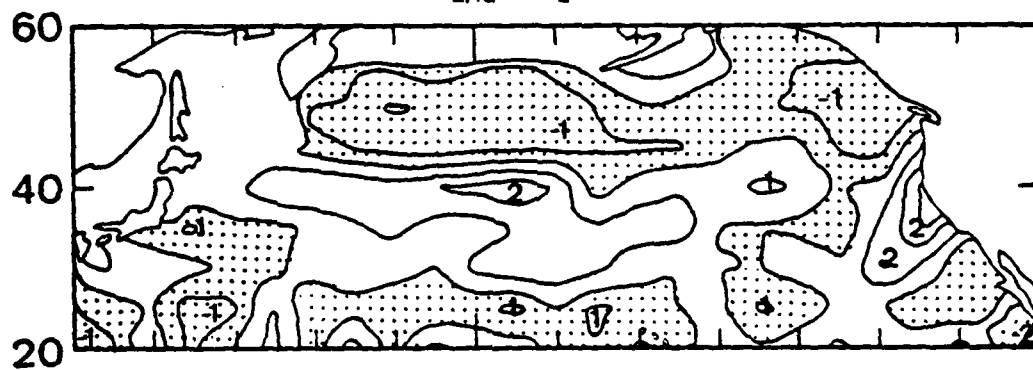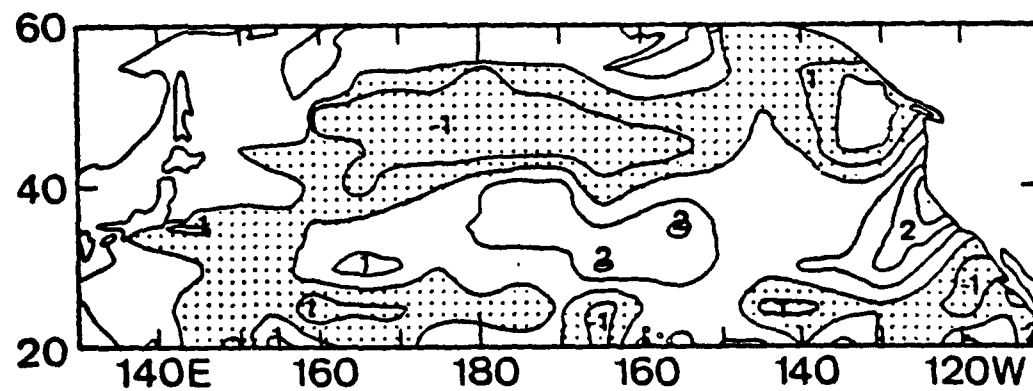
Figure 15. Same as Fig. 3 except for $(CURL_z\tau)HL$.

$(CURL_Z\tau)HL$

LAG = 0
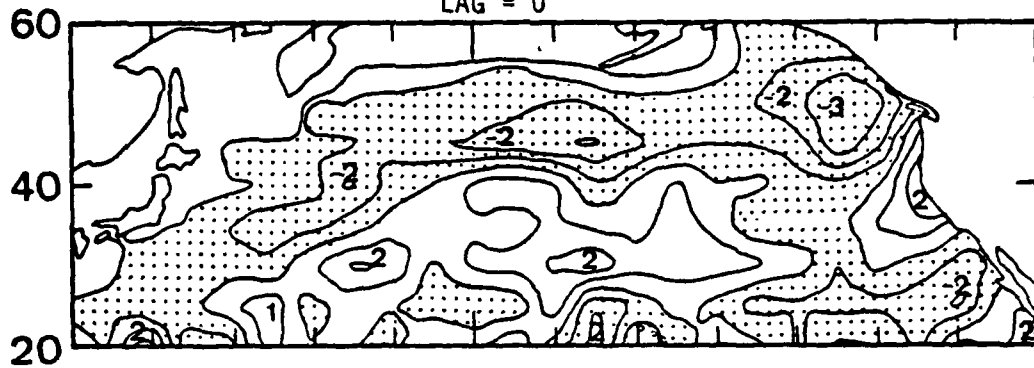
LAG = +1
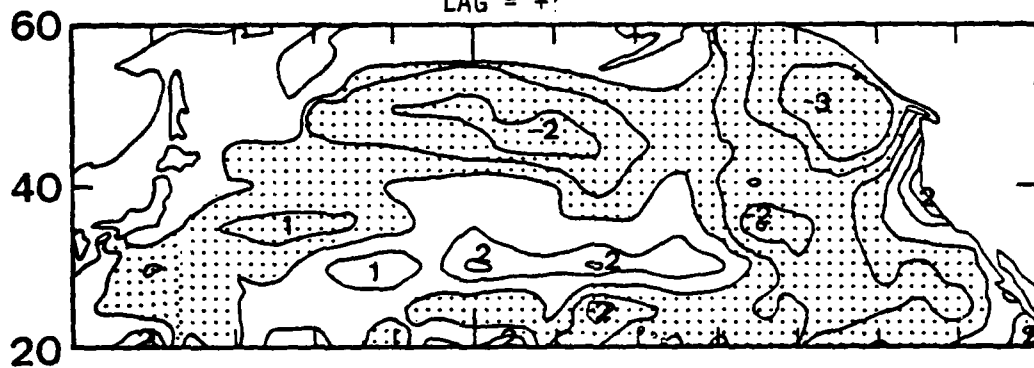
LAG = +2
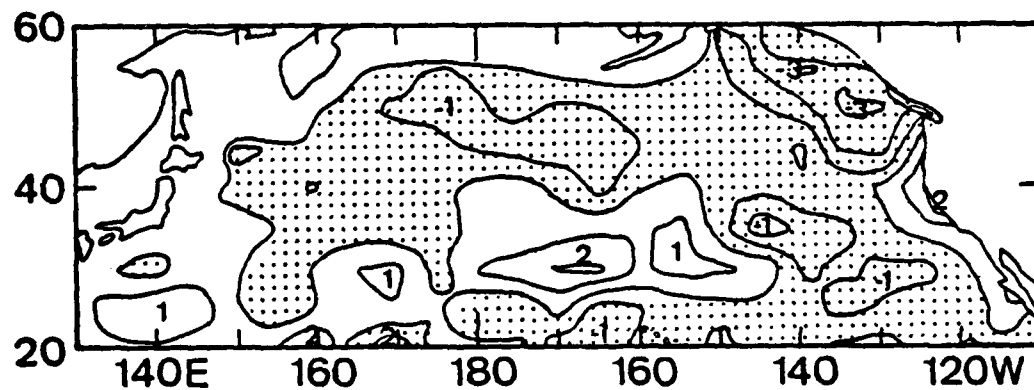
Figure 16. Same as Fig. 15 except for 0, +1 and +2 month lags.

38

$$(CURL_Z\tau)HL$$
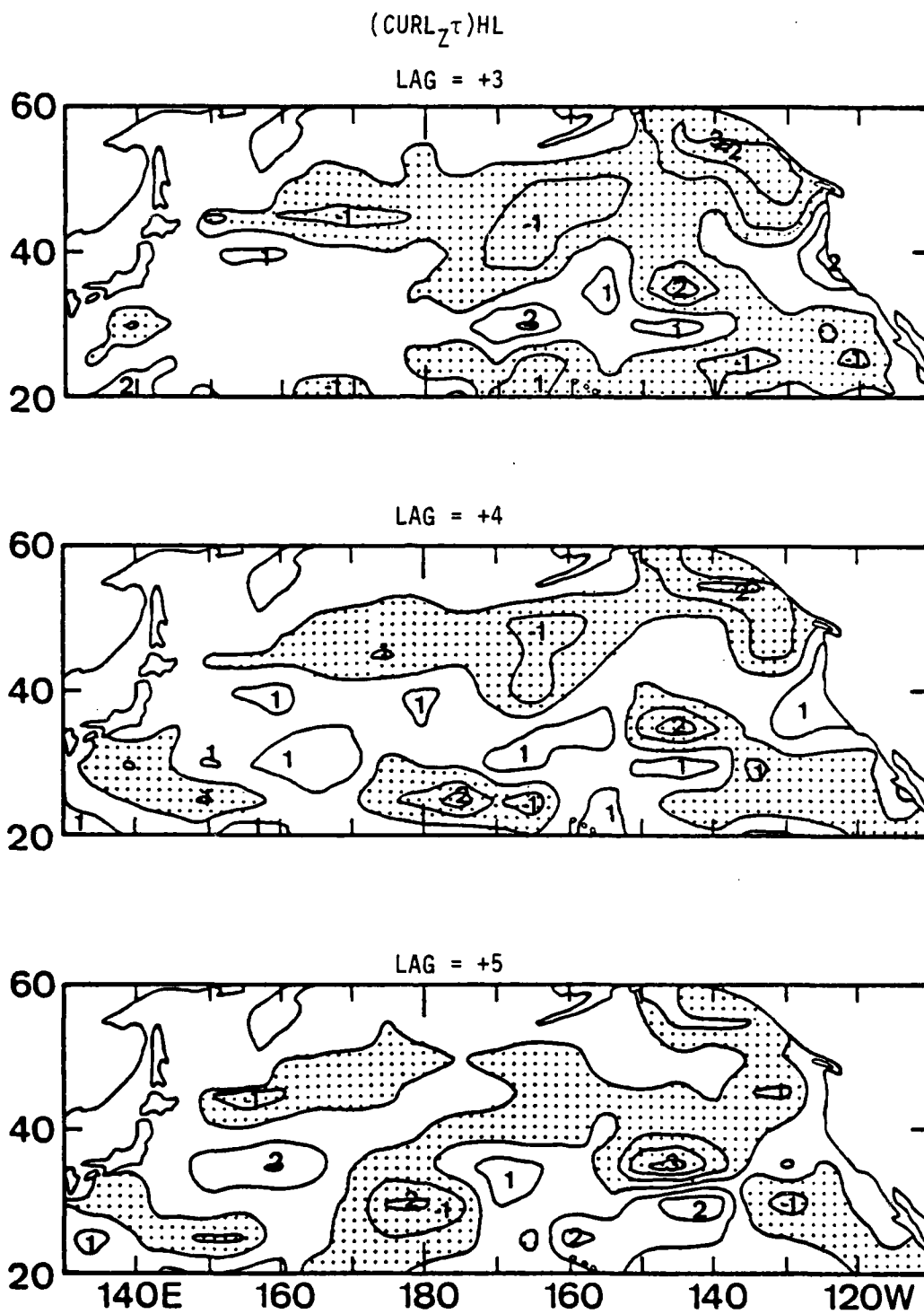
LAG = +3

LAG = +4

LAG = +5

Figure 17. Same as Fig. 15 except for +3, +4 and +5 month lags.

39
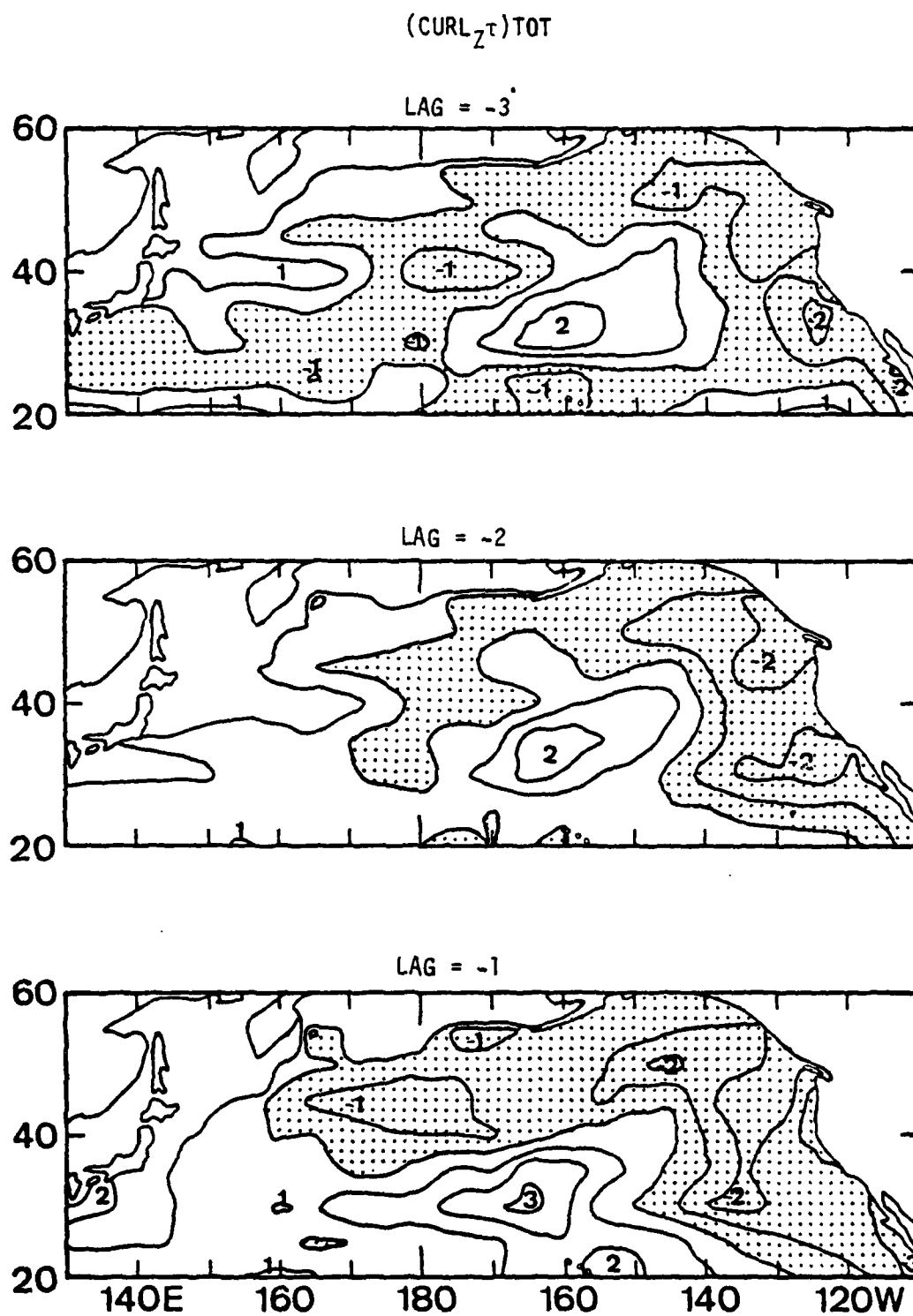
$(CURL_Z\tau)TOT$

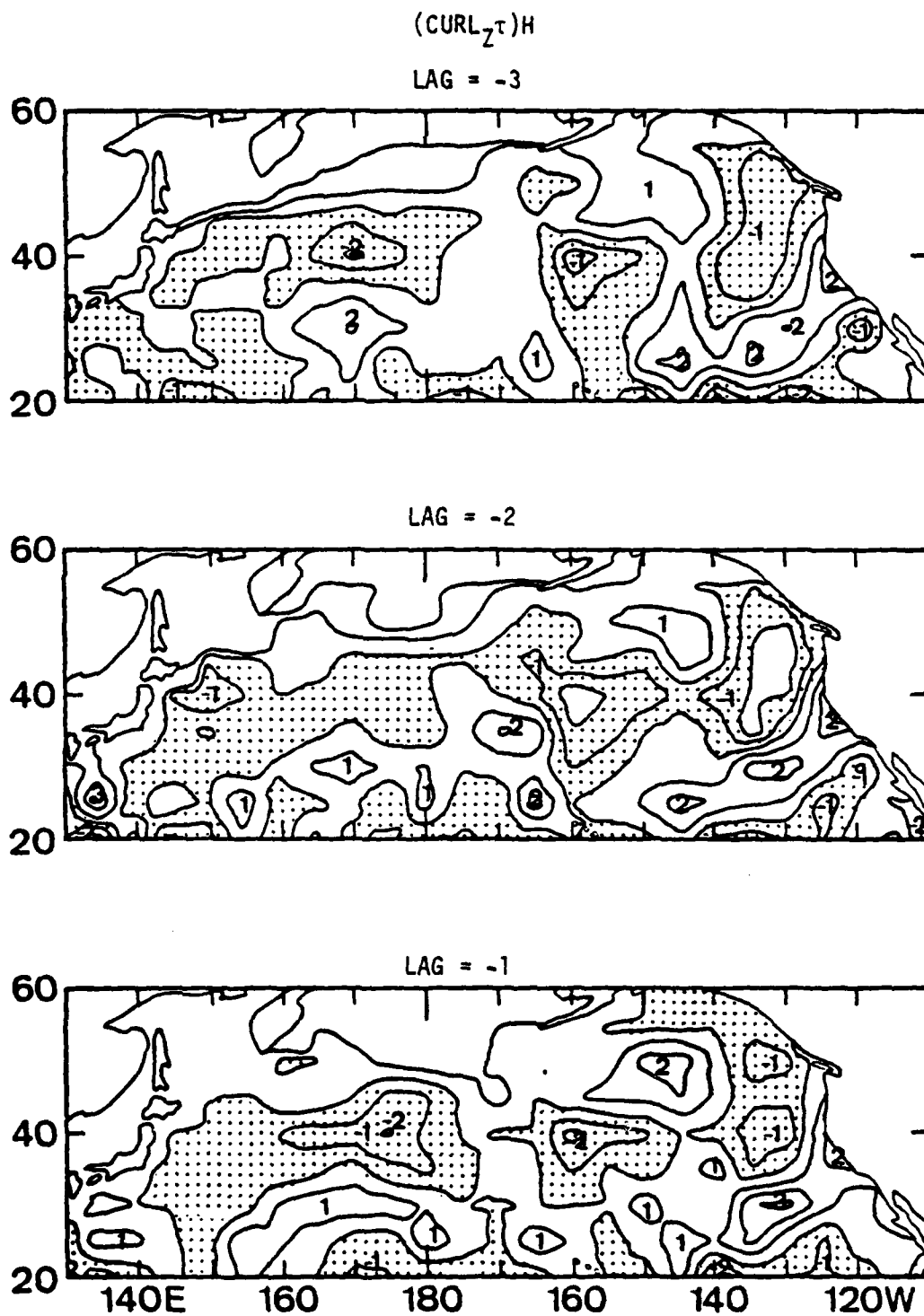Figure 18. Same as Fig. 3 except for $(CURL_Z\tau)TOT$.

40
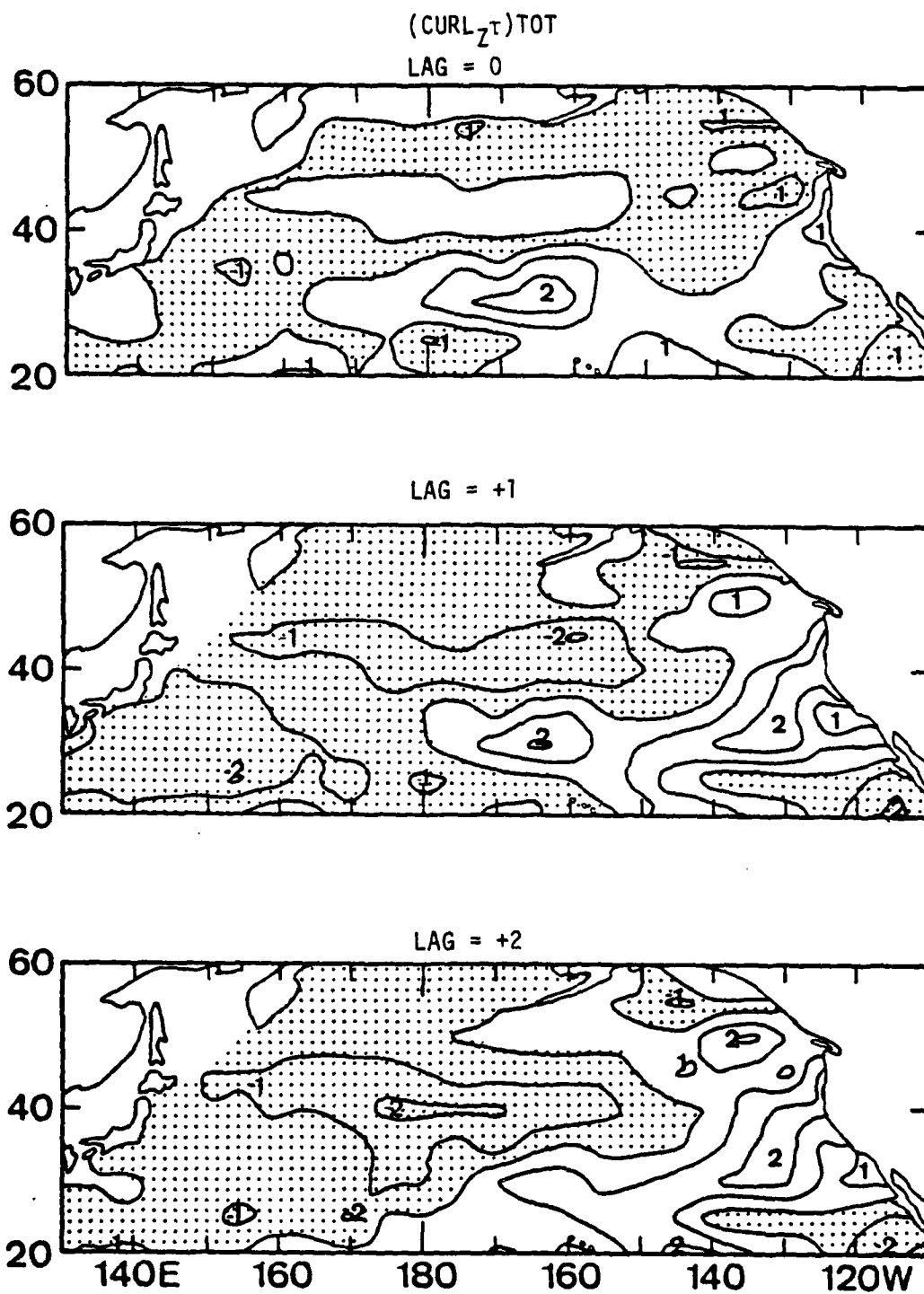
Figure 19.   Same as Fig. 18 except for 0, +1, and +2 month lags.

41

$(CURL_Z\tau)TOT$
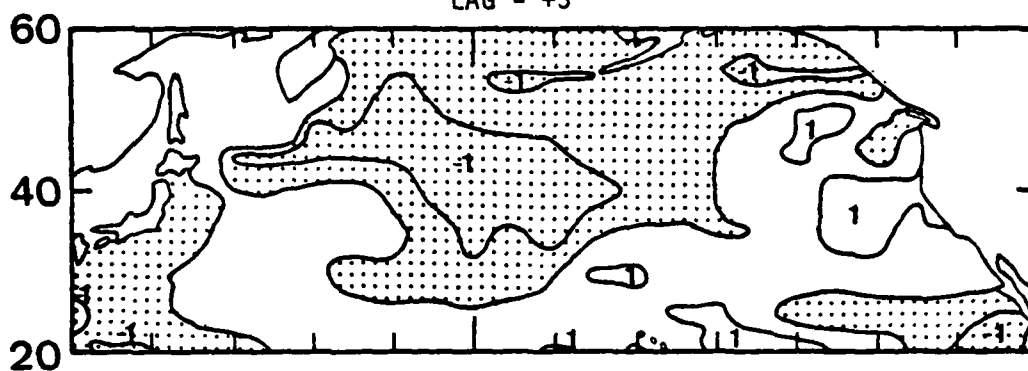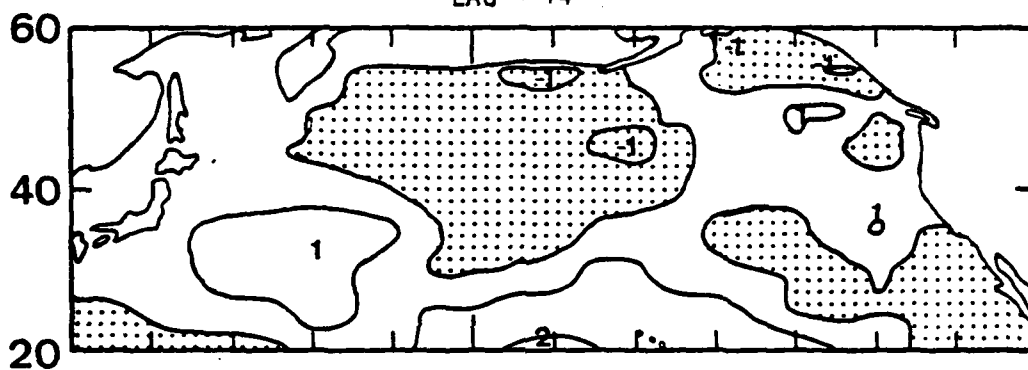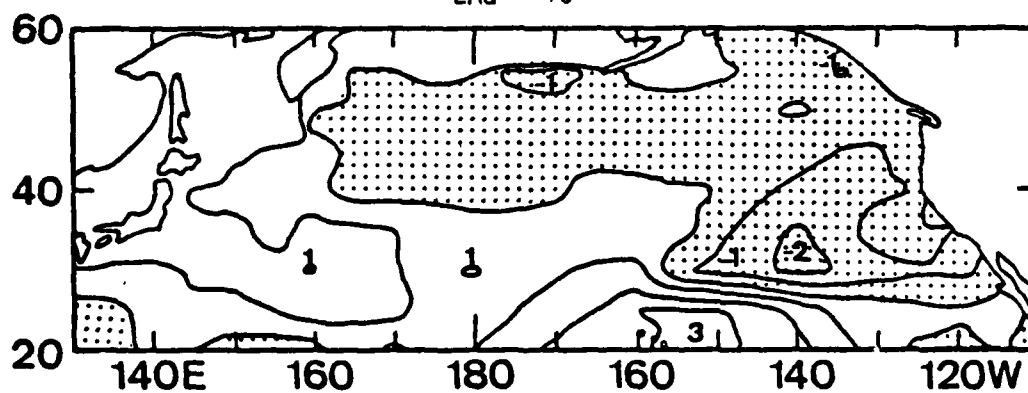
Figure 20. Same as Fig. 18 except for +3, +4 and +5 month lags.

42

magnitude 2 and 3 occur at (nearly) all lags for all three curl parameters with the most significant ones being those in the Gulf of Alaska and westward along the Aleutian Chain in Figure 16 (0 and +1 lag). This pattern is consistent with storm induced Ekman pumping cooling the SST. Another area which may, perhaps, be significant is seen at the plus one- and plus two-month lags in Figure 19. A positive correlation area, trending northeast-southwest, occurs off the North American coast and indicates that positive SST anomalies occur after above normal wind stress curl. This sequence is contrary to that expected from Ekman pumping.

Examination of the above year round lag correlations between the six wind parameters and SST appears to indicate that in the midlatitude North Pacific Ocean there is significant correlation of $(U_*^3)H$ and $(U_*^3)HL$ with SST for lags zero-to plus three-months.

3. Correlations Involving $\partial/\partial t$ SST

In an effort to further determine the data sets which provide the most significant correlations, the time rate of change of SST, $\partial/\partial t$ SST, over a two month period was calculated along with a two month average value for each of the three friction velocity and wind stress curl parameters. The resulting data sets (each 119 months long) were used to calculate raw cross correlations (at zero lag) which, in turn, were normalized by the large lag standard error calculated from the appropriate fields using (1). Figure 21 shows the normalized correlations between $\partial/\partial t$ SST and the three wind stress curl parameters and Figure 22 shows the normalized correlations between $\partial/\partial t$ SST and the three (U_*^3) parameters. Examination of Figure 21 reveals a rather large

43
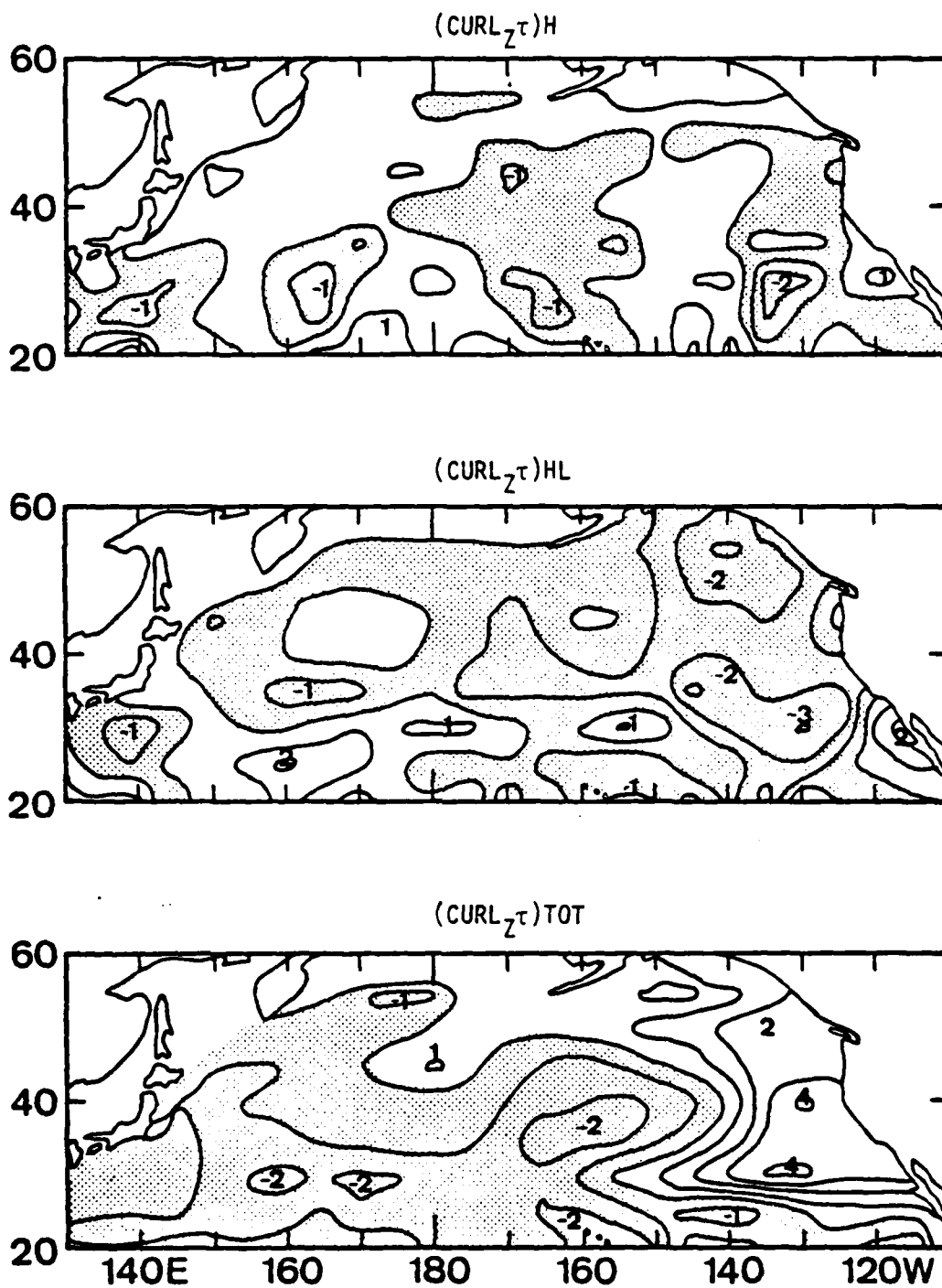
Figure 21. Normalized correlations at zero lag between $\partial/\partial t$ SST and $(CURL_Z\tau)H$, $(CURL_Z\tau)HL$ and $(CURL_Z\tau)TOT$. Contour interval is 1 and shaded areas denote negative correlations.

44
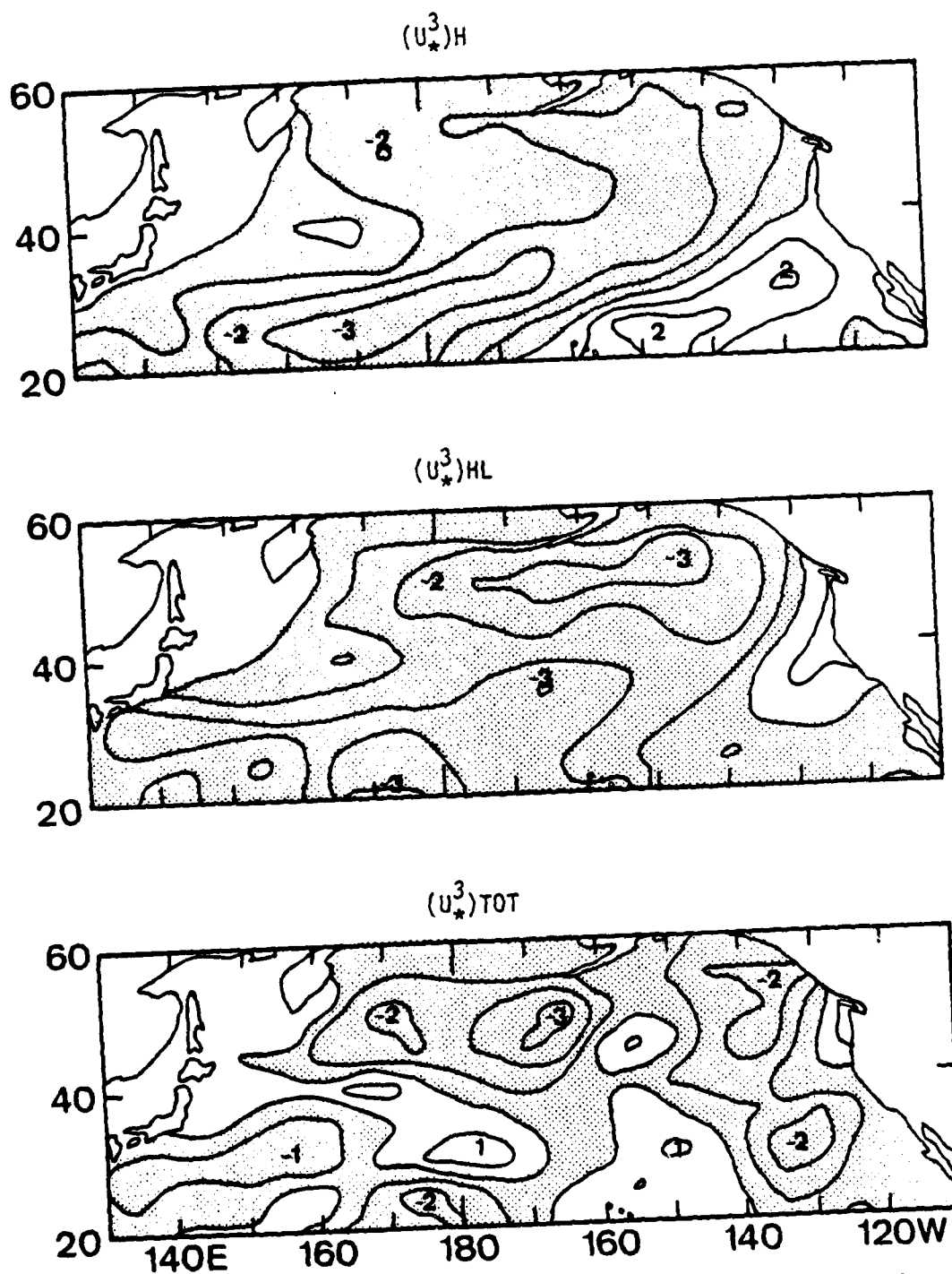
Figure 22. Same as Fig. 21 except for $(U_*^3)H$, $(U_*^3)HL$ and $(U_*^3)TOT$.

region of strong positive correlation between $\partial/\partial t$ SST and $(CURL_Z\tau)TOT$ trending northeast-southwest off the North American coast. This area appears to indicate a region where positive wind stress curl correlates with positive $\partial/\partial t$ SST and is clearly opposite the results expected from Ekman dynamics.

Figure 22 shows large areas of significant correlations between $\partial/\partial t$ SST and both $(U_*^3)H$ and $(U_*^3)HL$, as was seen in the lag correlations with SST. Comparison of the top and middle maps indicates improved correlation values in the Gulf of Alaska region due to the presence of the existing mean flow. The two storm related parameters clearly correlate better with $\partial/\partial t$ SST than the total (U_*^3) parameter. The better of the two parameters is considered to be the friction velocity computed from High- and Low-pass filtered components since it includes the synoptic storm activity in the presence of the existing mean flow, and in practice is nearly 5 times larger than $(U_*^3)H$ (Haney, Risch and Heise, 1981). For this reason, the $(U_*^3)HL$, SST and $\partial/\partial t$ SST data sets are used in the next section to investigate the possibility of a seasonal dependence in the air-ocean relations.

IV. SEASONAL RELATIONSHIPS BETWEEN (U_*^3)HL AND SST

Examination of the year-round relationships between (U_*^3)HL and SST
in the previous section showed significant correlations for the zero-to
plus three-month lags. It was further desired to determine if any
seasonal variation existed in these correlations. For example, one
might expect the SST anomaly to be more highly correlated with (anoma-
lous) atmospheric forcing in late summer, when the mixed layer is
shallowest, than in late winter, when it is deepest.

Two approaches to investigate the possible existence of seasonally
dependent relationships were considered. In the first approach (Section
A below), the correlations between monthly anomalies of SST and (U_*^3)HL
were calculated for each of the 12 starting months of January to
December and for lags of minus three-to plus five-months. The use of
correlations that depend upon the starting month provides information
on the seasonal variation of the wind-SST relationships, while the use
of lag correlations provides information on the time scales of the
events. As suggested above, one might expect larger correlations to
occur when the starting months are the summer months (June, July, August).
During this time of the year, the climatological ocean mixed-layer
depth is considered to be the shallowest. Anomalous storm activity
could, perhaps, more easily bring cooler water from below the mixed layer
and cause cooler SST values. On the other hand, one might expect less
significant correlations when the starting months are the winter months

47

(December, January, February). The climatological mixed-layer depth
is considered to be deepest at this time of the year and more intense
or more persistence storminess would, perhaps, be required to bring
cooler water from below the mixed layer. The lagged cross correlations
are first examined over the entire grid for each starting month and
lag, and then they are evaluated over a particular geographical area.

The second approach to examine for possible seasonal relationships
(Section B) tests the hypothesis given by

$$\partial/\partial t \ SST = - M(U_*^3)/(\alpha g h^2) \qquad (4)$$

where α is the thermal expansion coefficient, g is gravity, h is the
mixed-layer depth and M is a constant "tuning factor". Such a
hypothesis can be derived from simple mixed layer theory if the effects
of surface heating and cooling are neglected (see, for example, Denman
(1973), equation (18) and (25)). Two tests of this equation on a monthly
time scale are made using the $\partial/\partial t$ SST and (U_*^3)HL anomaly data sets.
In the first case, h is taken to be a constant, while in the second case
it is prescribed to vary regularly each year over the annual cycle.
The key question examined in Section B below is whether the use of
such a seasonally varying mixed-layer depth significantly influences
the normalized correlations between the parameters on the left and right
hand sides of (4).

48

A. SUBSAMPLE RECORD CORRELATIONS BETWEEN (U_*^3)HL AND SST

   1. Calculations Performed

      To investigate the possibility of a seasonal dependence in the
air-ocean relations, the complete 120-month records of (U_*^3)HL and SST
anomalies were divided into sub-sample records. Twelve separate records
were constructed - one for each of the months January through December -
with each record containing the ten anomaly values (one from each year)
for that month. For example, the first sub-sampled record of SST con-
tained the SST monthly anomaly values for January 1969, January 1970,
etc to January 1978. The second sub-sampled record contained the
monthly anomaly values for all ten February's, and so on. The (U_*^3)HL
records were treated similarly. The sampling interval in the sub-sample
records was 12 months, whereas the interval for the complete record was
one month.

      a. Raw Correlations

         Raw cross correlation values between SST and (U_*^3)HL were com-
puted from each of the 12 monthly records for lags of minus three-to
plus five-months. For example, a zero lagged correlation for the start-
ing month of January includes the cross correlations obtained from the
January 1969 SST and January 1969 (U_*^3)HL; January 1970 SST and January
1970 (U_*^3)HL; etc to January 1978 SST and January 1978 (U_*^3)HL. The
number of realizations for this January zero lag correlation is ten.
When considering January at plus five-months lag, for example, the cross
correlations are obtained from the January 1969 (U_*^3)HL and June 1969 SST;
January 1970 (U_*^3)HL and June 1970 SST; etc to January 1978 (U_*^3)HL and
June 1978 SST and the number of realizations is ten. For negative

49

correlations the number of realizations is nine. Thus there are typically

nine or ten realizations in the seasonal lagged correlations compared

to 115 to 120 realizations for the lagged correlations based on the

complete record.

The seasonal lagged raw cross correlation values ranged

from 0.2 to 0.8 with a large percentage of them between 0.5 and 0.7.

This can be compared with the complete record raw cross correlations

in which the range was from 0.1 to 0.3 with a large number near 0.2.

The increase is largely due to increased artificial correlation as is

shown below.

b. Significance Levels

The question of statistical significance must once again be

considered and in order to evalute the significance levels, seasonal

values of the large lag standard errors were calculated for individual

lags and starting months. The σ_K values are very dependent upon record

length. Reduction of the sample size from typically 120 for the com-

plete record to typically ten for the sub-sample record causes an

increase in σ_K from a value of approximately 0.1 to values ranging from

0.3 to 0.4. The expected artificial correlation, σ, increased by a

factor of (approximately) $\sqrt{12} = 3.46$ as the record length (or number of

realizations) was decreased by a factor of (approximately) 12. Evalua-

tion of the bivariate integral time scale, $\hat{\tau}$, given by (3), becomes

more difficult due to the less well-behaved nature of the autocorrela-

tion functions which were computed for all i in the range $-23 < i < 23$

(Figure 23). The criteria of successive values of $\hat{\tau}$ changing less than

1% as the summation limit I was increased by 1, could not be achieved,

50
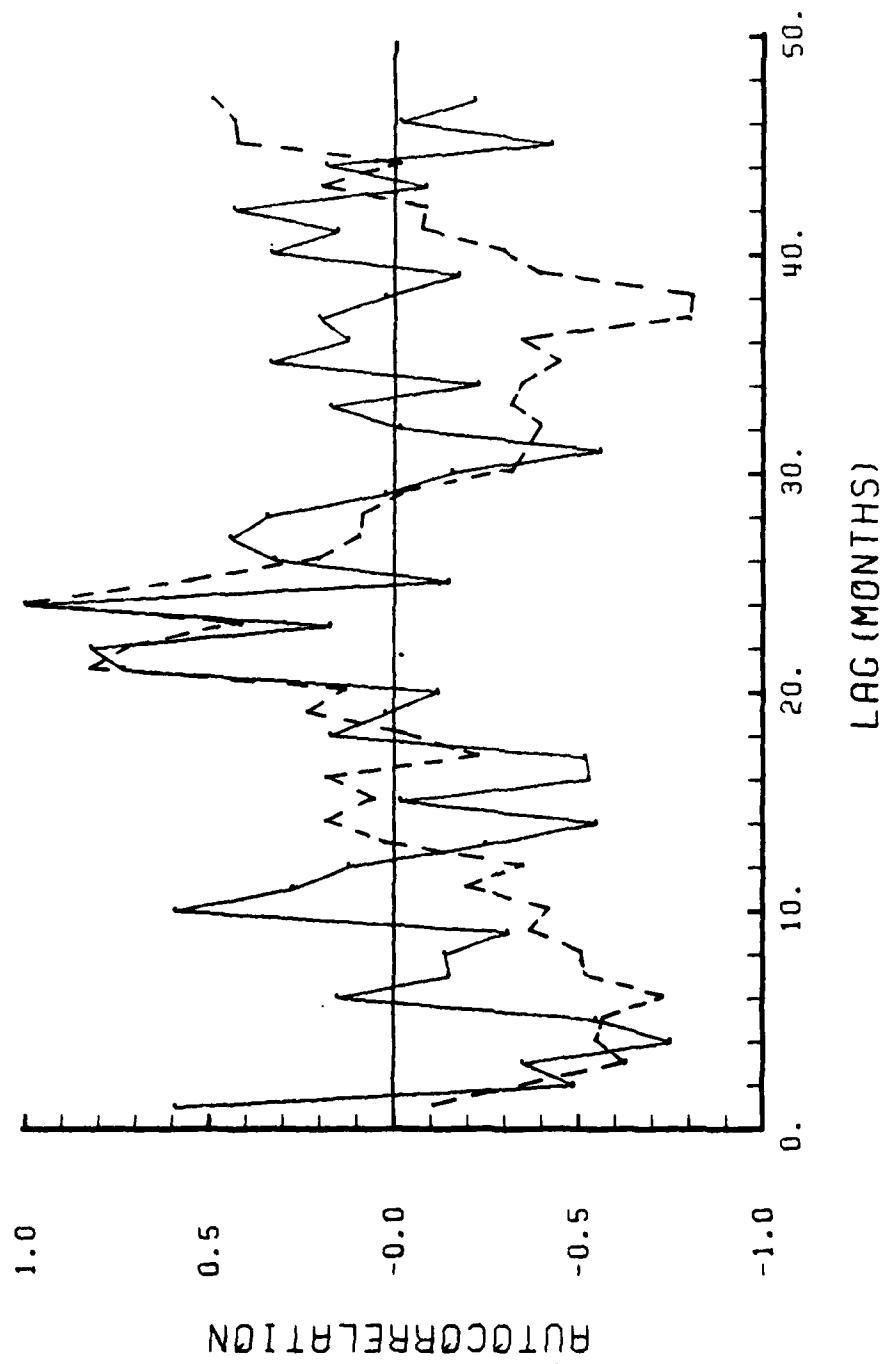
Figure 23. SST (dashed) and $(U_*^3)HL$ (solid) autocorrelation functions vs lag based on sub-sample records.

51

even for the maximum summation limit $I=23$. For this reason, the large

lag standard error in the present case of the sub-sampled record was

estimated by $\sigma_K^* = \sqrt{12}\ \sigma_K$, where σ_K is given by (2) and calculated from

the complete record. The σ_K^* values thus computed were (approximately)

0.35 and were spatially coherent over the entire grid area. As an

example, Figure 24 shows σ^* values for the zero lag case.

The raw lagged correlations at each grid point for each

of the 12 starting months were normalized by the σ^* value for that

grid point, yielding normalized lagged correlations on the order of

1 to 2 as shown below.

2. Results

a. Lag Correlations between (U_*^3)HL and SST

Figures 25 to 28 are maps of normalized correlations between

monthly anomalies of (U_*^3)HL and SST at plus one-month lag and starting

months of January through December. The correlations for the starting

months of January, February, and March are shown in Figure 25, while

the other starting months are in Figures 26 to 28. In each map, shaded

areas are indicative of negative correlations (e.g. above normal stormi-

ness, (U_*^3)HL, followed one month later by below normal SST) and the

contour interval is 1.

Examination of the map series reveals negative correlations

over large areas of the grid. This result agrees with the results

from the complete year-round record and is consistent with the hypothesis

that anomalous storminess produces subsequent cooling. The significance

levels, however, are not as large due to the increased value of σ_K^* over
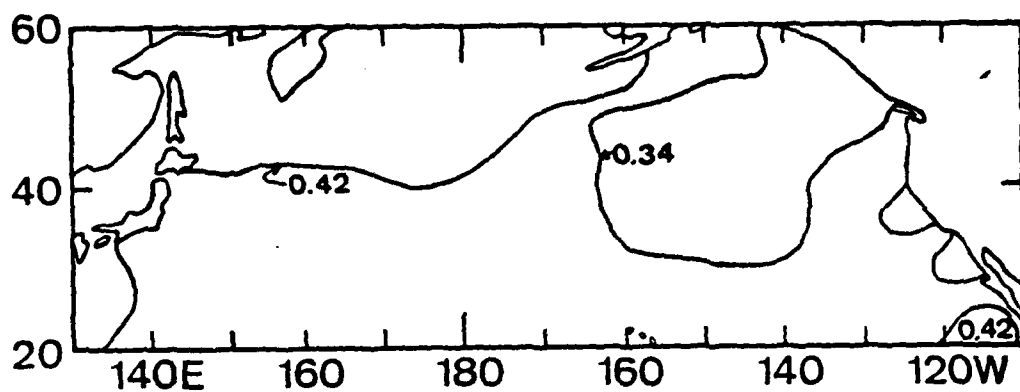
Figure 24. Zero lag σ^* values for the variables SST and (U_*^3)HL. Contour interval is 0.08.

$(U_*^3)HL$

JANUARY
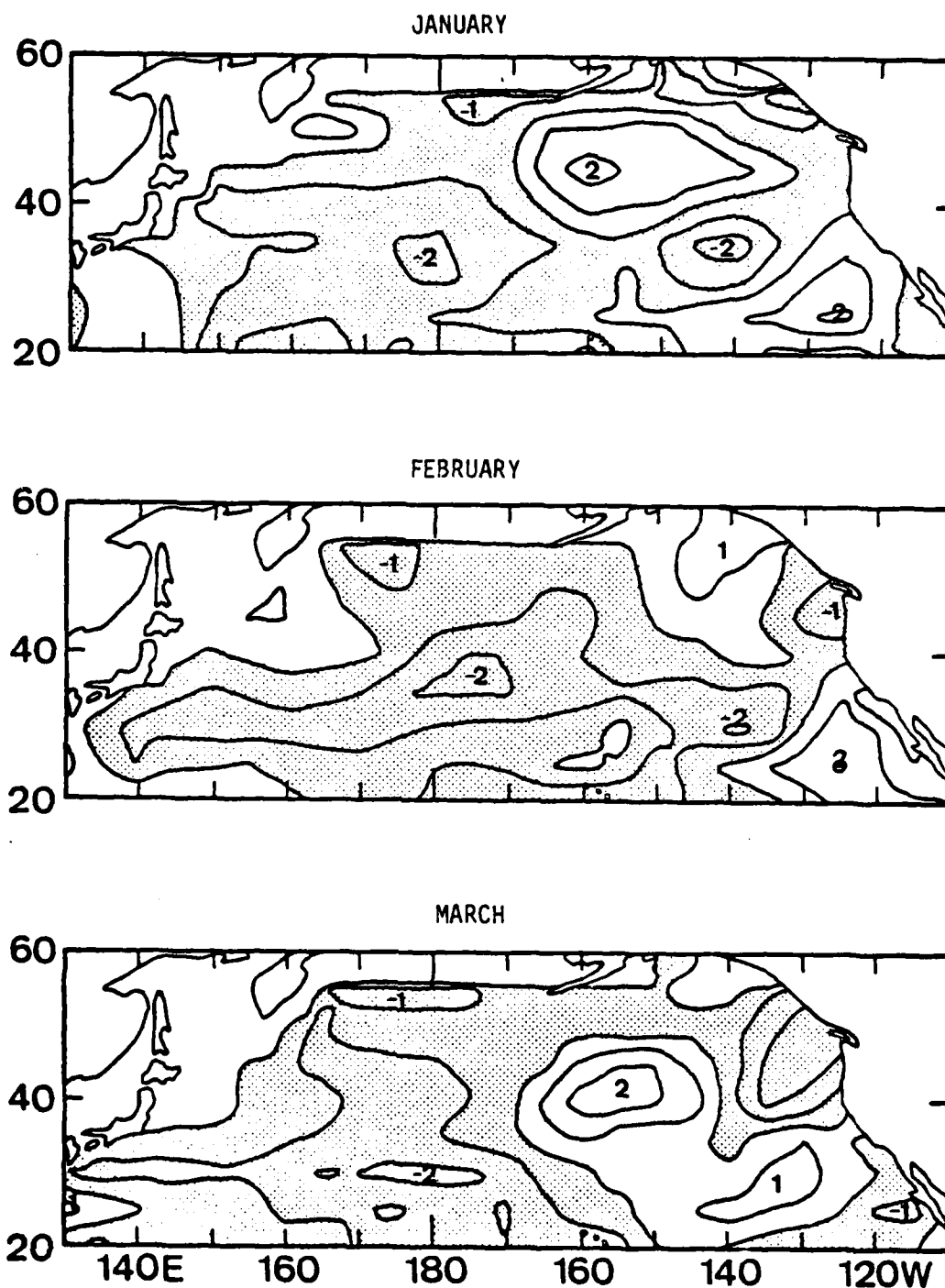
FEBRUARY

MARCH

Figure 25. Subsample record correlations (nondimensionalized by
σ_K^*) between SST and $(U_*^3)HL$ for +1 month lag and
starting months January (top), February (middle),
and March (bottom). Contour interval is 1 and shading
indicates negative correlations.

54
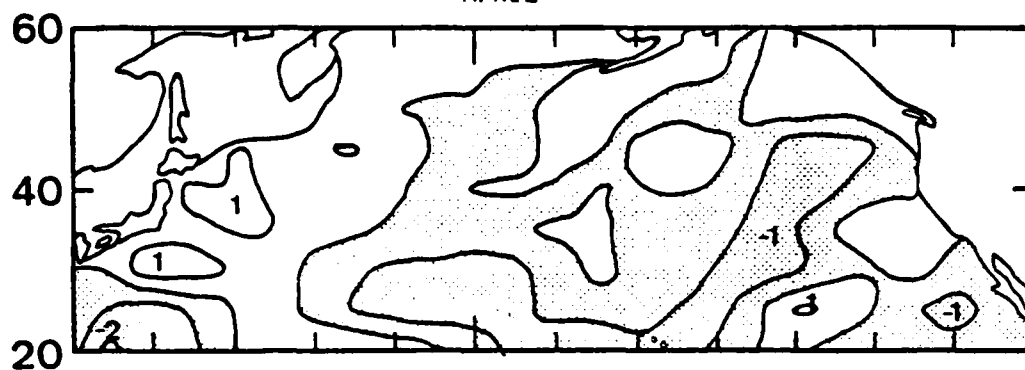
$$(U_*^3)HL$$

APRIL

MAY

JUNE
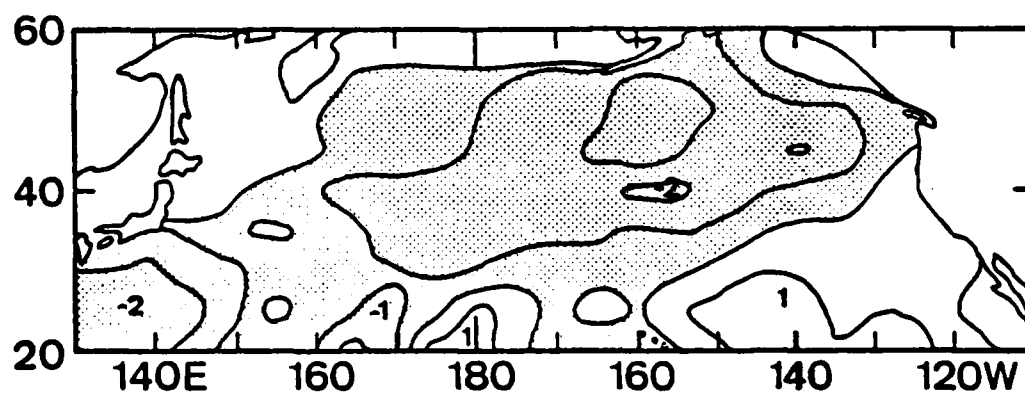
Figure 26.   Same as Fig. 25 except for April, May and June.

$(U_*^3)HL$

JULY
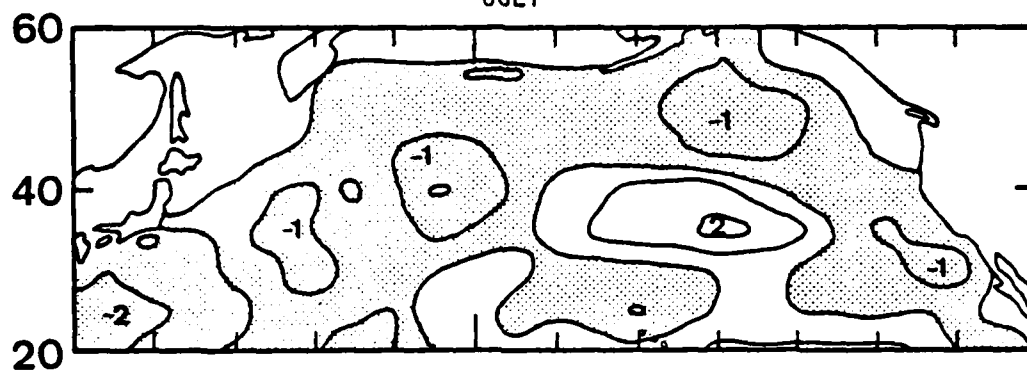
AUGUST

SEPTEMBER
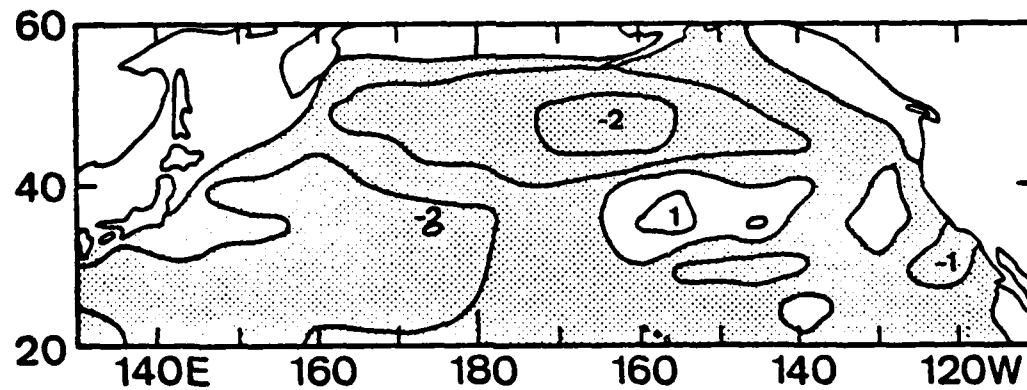
Figure 27. Same as Fig. 25 except for July, August and September.

$(U^3_*)HL$
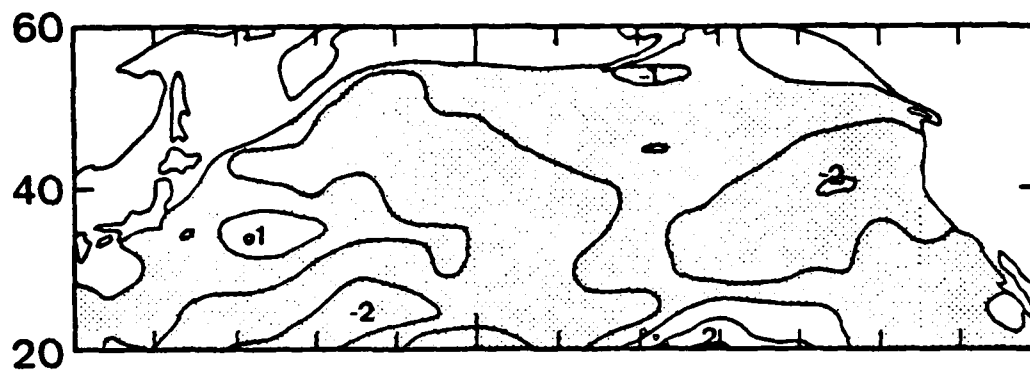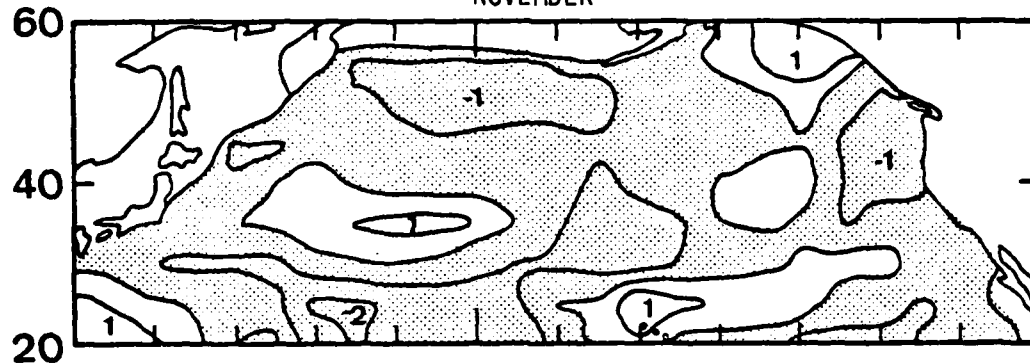
OCTOBER

NOVEMBER

DECEMBER
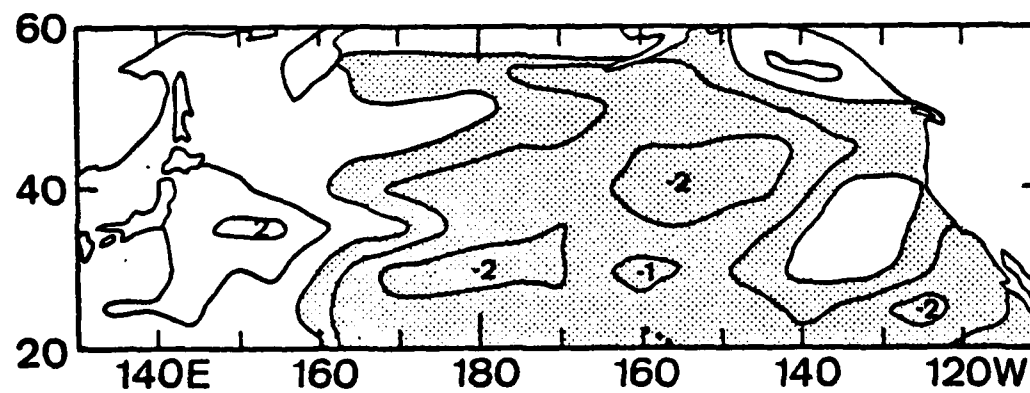
Figure 28. Same as Fig. 25 except for October, November and
December.

57

σ_K. It was felt that the existence of a seasonality in the relation-ships between (U_*^3)HL and SST would be evidenced in the map series by one starting month, or perhaps a series of starting months having clearly higher (nondimensional) correlations than the rest. Figures 25 to 28 do not show such a result and appear to show less areas of magnitude 2 and 3 and thus less significance than the complete year-round record. Further investigation into the seasonality was done by considering a specific portion of the grid or an index area.

b. Central North Pacific Ocean Index Area

An open ocean index area consisting of 18 grid points cover-ing the area 30° N to 40° N and 170°E to 165° W was chosen to further consider the question of seasonality since this region contained the most significant correlations based on the complete year-round record. An average normalized correlation over the index area was computed from *the map series in the* previous section for each starting month from January through December and all lags from minus three-to plus five-months (Table I). The values in Table I for the zero and positive lags are nearly all negative. The magnitudes, however, are nearly all less than 2. This is less significant than the average value (at one month lag) of -2.84 obtained for the index area using the complete year-round record. A graphical presentation of the seasonal correlations for zero-, plus one-, and plus two-month lags (Figure 29) appears to indicate that the most significant (negative) correlation between (U_*^3)HL and SST, averaged over the index area, occurs during the winter months December, January, and February, whereas the least significant relationships occur

58

STARTING MONTH	-3	-2	-1	0	+1	+2	+3	+4	+5
JAN	.75	-.22	-.31	-.65	-1.39	-1.13	-1.39	-.83	.79
FEB	-.31	-.88	-.48	-1.42	-1.27	-1.25	-.66	.05	-.14
MAR	.07	.31	.51	-.33	-1.10	-.82	-.74	-.07	.42
APR	-.32	-.05	-.63	-1.00	-.51	-.08	-.06	-.11	-.58
MAY	-.29	-.05	.37	-.39	.33	-.16	-.06	-.11	-.58
JUN	.81	.56	1.02	-1.07	-1.23	-.56	-.70	-1.05	-1.34
JUL	.51	.33	-.72	-.67	-.35	-.74	-.63	-.75	-.19
AUG	.78	-.42	-.51	-1.02	-.39	-.87	-1.22	-1.15	-.77
SEP	.10	.19	-.42	-.84	-.89	-.71	-.67	-.70	-1.04
OCT	-.23	-.76	-.26	-1.00	-1.32	-.77	-.38	-.44	-1.00
NOV	-.27	-.05	-.19	-.94	-.41	-.69	-1.16	-1.31	-.89
DEC	-.11	-1.25	-1.55	-1.83	-1.68	-1.29	-1.43	-1.50	-1.40

LAG(K)

Table I. Nondimensional Index Area correlations calculated from the sub-sample record as a function of starting month and lag. The nondimensionalization is done using $\sigma_K^* = \sqrt{12}\,\sigma_K$, with σ_K calculated from (2).
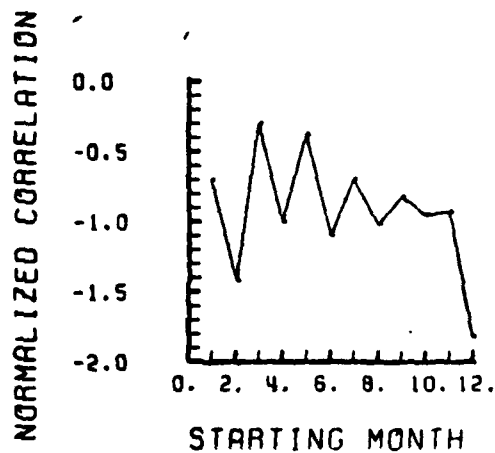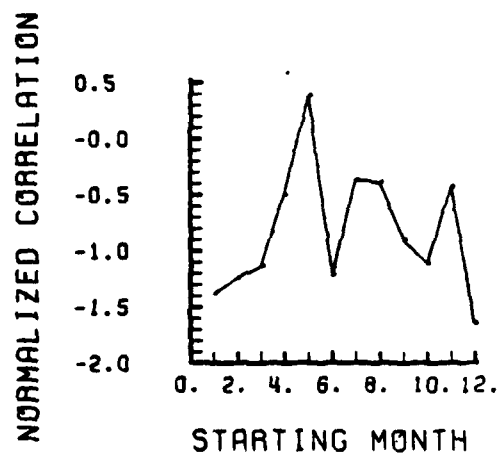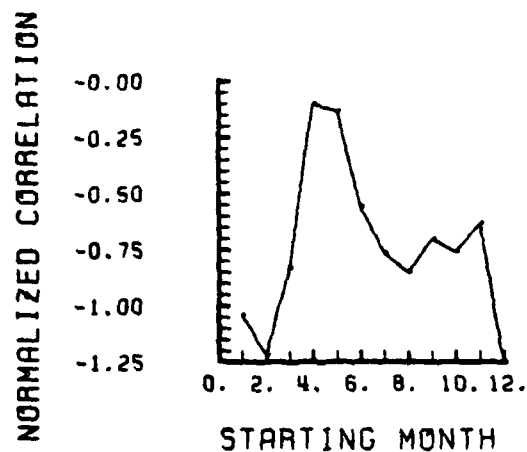
Figure 29. Plot of normalized seasonal correlations between the variables SST and (U_*^3)HL averaged over the Gulf of Alaska Index Area. Lags of zero (top), plus one (middle) and plus two (bottom) months are shown.

60

in the summer months of June, July and August. This is different from the expected result noted above.

Because of the generally low significance of these correlations and their variation during the year and the fact that the index area was chosen a priori on the basis of significant year-round correlations, it is felt that no firm conclusion can be drawn from the results of this section. That is, it cannot be stated with any statistical confidence whether or not there is a seasonal variation in the lag correlations. In order for this method of sub-sampled record analysis to be fruitful, a much longer total record length is required.

B. MODEL TESTS

1. Correlations

The second approach to investigating seasonal relationships between (U_*^3)HL and SST was one of a test of the hypothesis given by (4), with particular attention to the effect of a seasonally varying mixed-layer depth. The time rate of change of SST over a two month period and the average (U_*^3)HL over the same two month period were calculated from the complete 120-month record. The resulting 119-month records were used to compute correlations in which two cases were considered.

In the first case, the mixed-layer depth, h, was held constant over the entire record. Raw cross correlations for each of the 166 grid points were calculated between the two data sets and normalized using the large lag standard error, σ, for the 119-month record given by (1). Typical values of σ were 0.07 to 0.09 with all values less than 0.1. The resulting normalized correlations ranged in magnitude from 1 to 3, as shown previously in Figure 22 (middle) and discussed further below.

61

In the second case, the mixed-layer depth, $h(t)$, is prescribed to vary according to

$$h(t) = H + \Delta H \cos \left(\frac{2\pi(t-t_0)}{12}\right) \qquad (5)$$

where $H = 75m$ represents an annual average mixed layer depth, $\Delta H = 50$ m represents the amplitude of the seasonal variation and t_0 its phase. In (5), t runs from 1 to 120 months. This function allows the mixed-layer depth to oscillate each year from a maximum of 125 m in month t_0 to a minimum of 25 m in month $t_0 = +6$ For example if $t_0 = 1$, the maximum depth occurs in January and minimum in July while if $t_0 = 2$, the maximum occurs in February and minimum in August. Raw cross correlations between $\partial/\partial t$ SST and $(U_*^3)HL/h(t)^2$ were computed and then normalized using the large-lag standard error calculated as in (1). Correlations were calculated for all values of the phase, t_0, from 1 to 12 allowing the deepest mixed-layer depth to occur successively in each of the 12 months.

2. Results

The middle map in Figure 22, presented in Section III, shows the normalized correlations between $\partial/\partial t$ SST and $(U_*^3)HL$. This represents a test of (4) and (5) with $\Delta H = 0$, i.e. constant h. Two areas of significant correlation (magnitude 2 and 3) occur in the figure and appear to support the hypothesis that positive values of anomalous storminess are well correlated with negative values of $\partial/\partial t$ SST. The nine grid points in the Gulf of Alaska region of Figure 22, which have

62

normalized correlation values of magnitude 3 or greater, were considered to investigate the influence of prescribing a seasonally varying mixed-layer depth.

Figure 30 shows the normalized correlation value, averaged over the Gulf of Alaska Index Area, and presented as a function of the phase of the mixed-layer depth. Figure 31 shows a similar plot for the Central North Pacific Ocean Index Area used earlier. Examination of Figures 30 and 31 reveals that, in general, very little increase in significance is obtained by the introduction of a seasonally varying mixed-layer depth. For both index areas, it appears that the chances of reducing the correlation is greater than the chances of increasing it. In addition, the phase of the mixed-layer depth that results in the best correlation is different for the two index areas. In the Gulf of Alaska Region (Figure 30) the best (most negative) normalized correlations occur when the mixed-layer depth is prescribed to be deepest in March (and shallowest in September), while the poorest (least negative) correlations occur in the case when it is deepest in August. In the Central North Pacific Ocean Region (Figure 31) the best normalized correlations occur in the case when the mixed-layer depth is deepest in December, whereas the poorest occur in the case when it is deepest in May or June. In both of these areas, the introduction of a seasonally varying h (even if optimized as to phase) does not improve the correlations. It thus appears that while there is (considerable) support (Fig. 22) for the hypothesis given by (4) (i.e. $\partial/\partial t$ SST and (U_*^3)HL negatively correlated) no significant improvement is obtained by the introduction of a seasonally varying mixed-layer depth to modulate the (U_*^3)HL term.

63
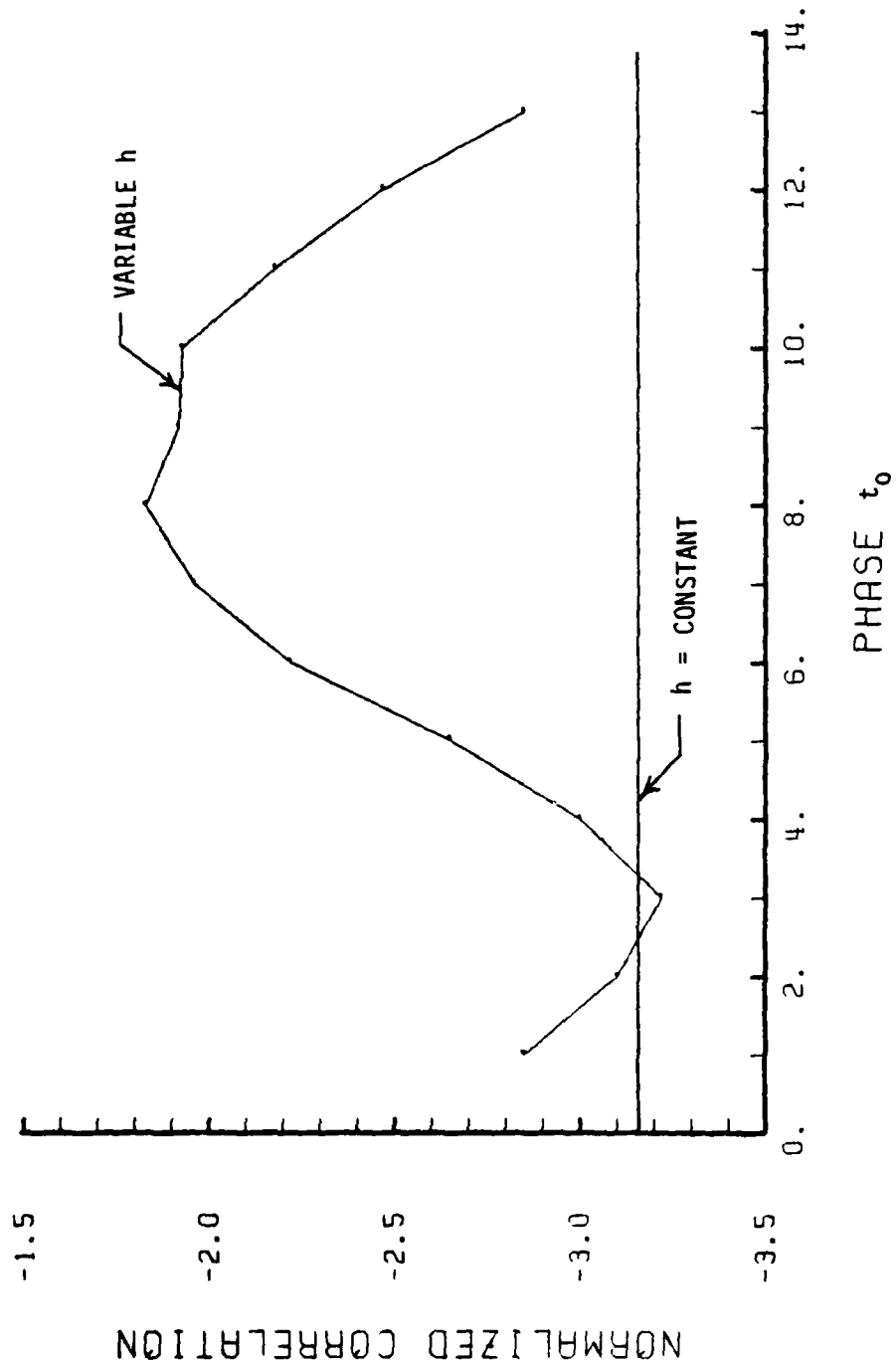
Figure 30. Normalized correlation, averaged over The Gulf of Alaska Index Area, vs phase, t_0, of the mixed-layer depth. The case of constant h (calculated from Fig. 22) is also shown.
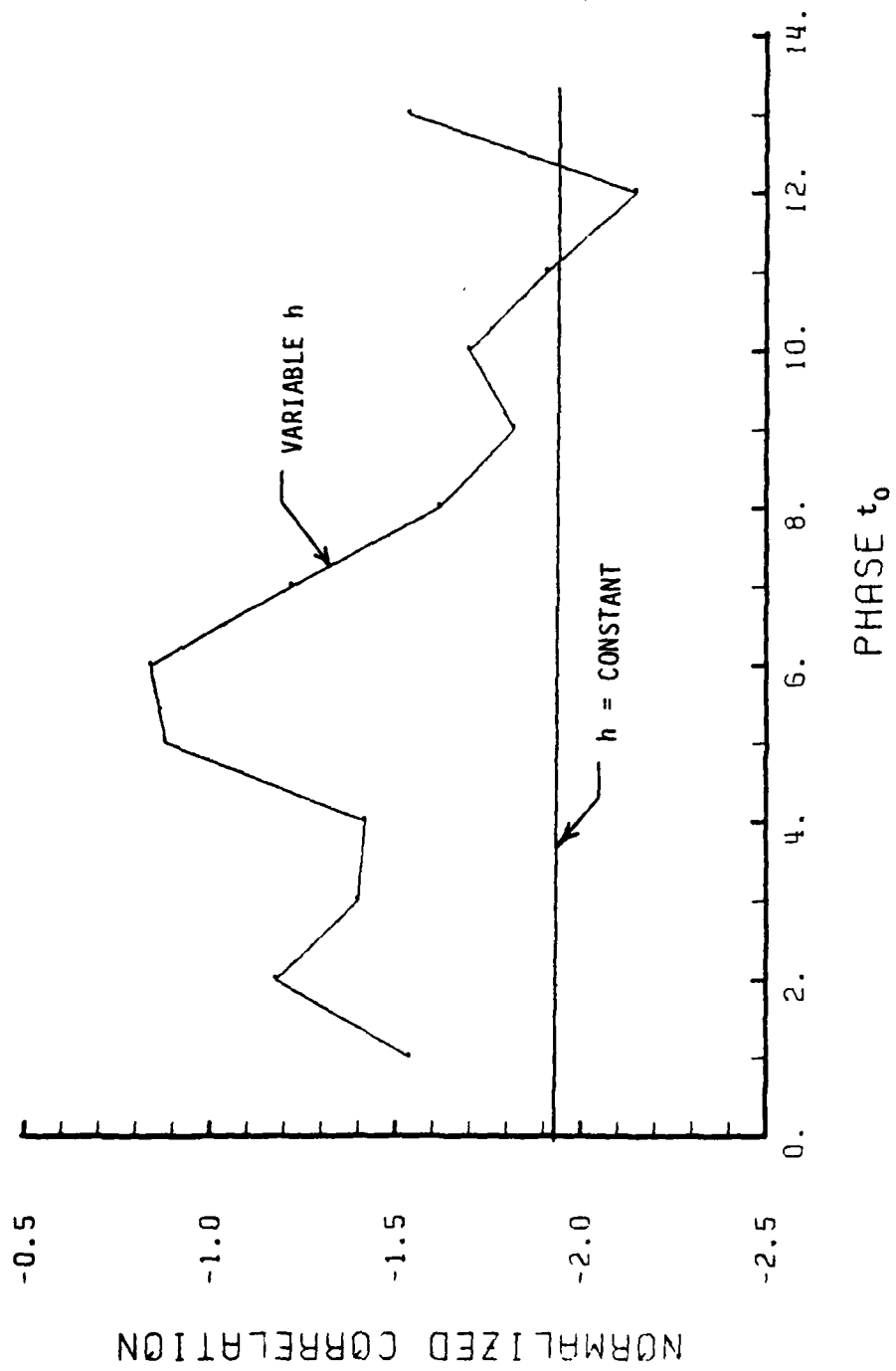
Figure 31. Same as Fig. 30 except for Central North Pacific Ocean Index Area.

In order to give additional observational support to the (statistically significant) year-round correlations found between synoptic storm activity, represented by $(U_*^3)HL$, and the development of monthly SST anomalies, represented by $\partial/\partial t$ SST, the synoptic developments observed during the Winter of 1977 are described in the next section.

V. SYNOPTIC RELATIONSHIPS

In an effort to gain further insight into the dynamics of the relationships between $\partial/\partial t$ SST and (U_*^3)HL, three questions were considered. First, are the best correlations between $\partial/\partial t$ SST and (U_*^3)HL occurring only when (U_*^3)HL is positive or only when it is negative, or are the correlations the same in both cases? Second, are there one or two particular cases or months in the ten-year time series when SST and (U_*^3)HL are extremely well correlated and if so, can this high correlation be seen by comparing the SST anomaly maps with conventional storm track data for the same time period? Third, are the best correlations in the North Pacific Ocean occurring along or displaced from the mean climatological storm track?

In considering the first question of positive or negative (U_*^3)HL values leading to the best correlations, the 119-month data records for $\partial/\partial t$ SST and (U_*^3)HL were utilized, with (U_*^3)HL being the key. For each of the 166 grid points and all t, $t = 1$ to 119, it was determined if the (U_*^3)HL anomaly at t was greater than zero, or not. The positive (U_*^3)HL anomalies at time t were correlated with the corresponding SST value (Figure 32). For positive (U_*^3)HL, large areas of negative correlation occur, indicating above normal storminess is correlated with decreasing SST ($\partial/\partial t$ SST < 0). Similarly, for negative (U_*^3)HL, large areas of negative correlation also occur indicating that below normal storminess is correlated with increasing SST ($\partial/\partial t$ SST > 0). Figure 32

67
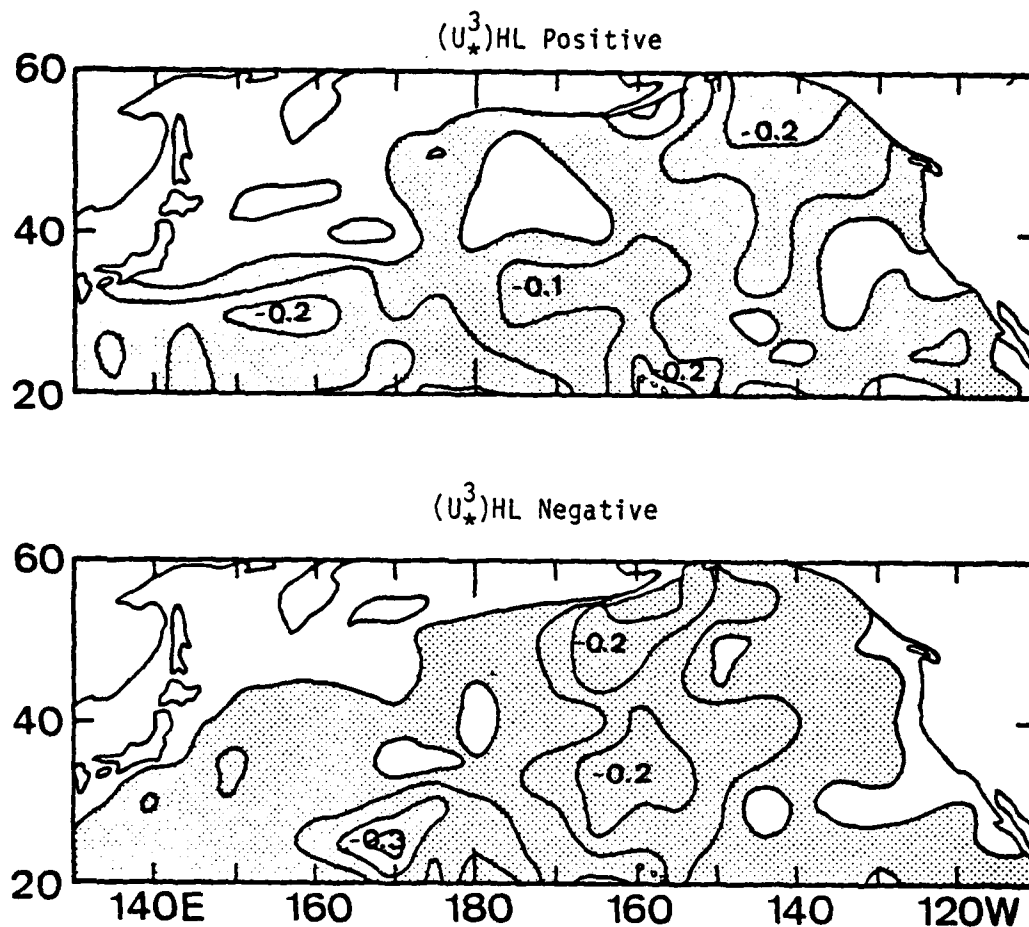
Figure 32. Correlations between (U_*^3)HL and $\partial/\partial t$ SST_3 for positive (top) and negative (bottom) values of (U_*^3)HL separately. Contour interval is 0.1 and shaded areas denote negative correlations.

68

appears to indicate little difference in the correlations among the two distributions. Both above normal and below normal values of $(U_*^3)HL$ correlate equally with $\partial/\partial t$ SST, with neither being clearly dominate. None of the correlations in Figure 32 are very significant on a purely statistical basis because the large lag standard error (artificial correlation) for these data sets are approximately $\sqrt{2}$ times that of the total record. Thus, raw correlations must be near 0.3 to be significant at the 95% confidence level.

To determine if there was a particular period in which SST and $(U_*^3)HL$ were extremely well correlated, the Gulf of Alaska Index Area described earlier was chosen for examination. The two time series for t = 1 to 119 were averaged over the index area and plotted in Figure 33. This figure, as much as any other, shows the short time scales (approximately 1 to 2 months) which lead to the estimate of 1/100 for the number of independent events in the record. It is because of the small σ values that a correlation of 0.3, while small, is highly significant. The sequence September, October, November 1977 was chosen for further examination because of the apparently good correlation at that time. The actual $(U_*^3)HL$ and SST anomaly values for each of the months September, October, and November were plotted and compared with the principal tracks of centers of cyclones at sea level, as given in Mariners Weather Log (1978) and the observed climatology of principal low tracks (Klein 1956). This was done in an attempt to see if the anomalies in $(U_*^3)HL$ could be related to the apparent "storm track anomalies". The results are shown in Figures 34, 35 and 36.

69
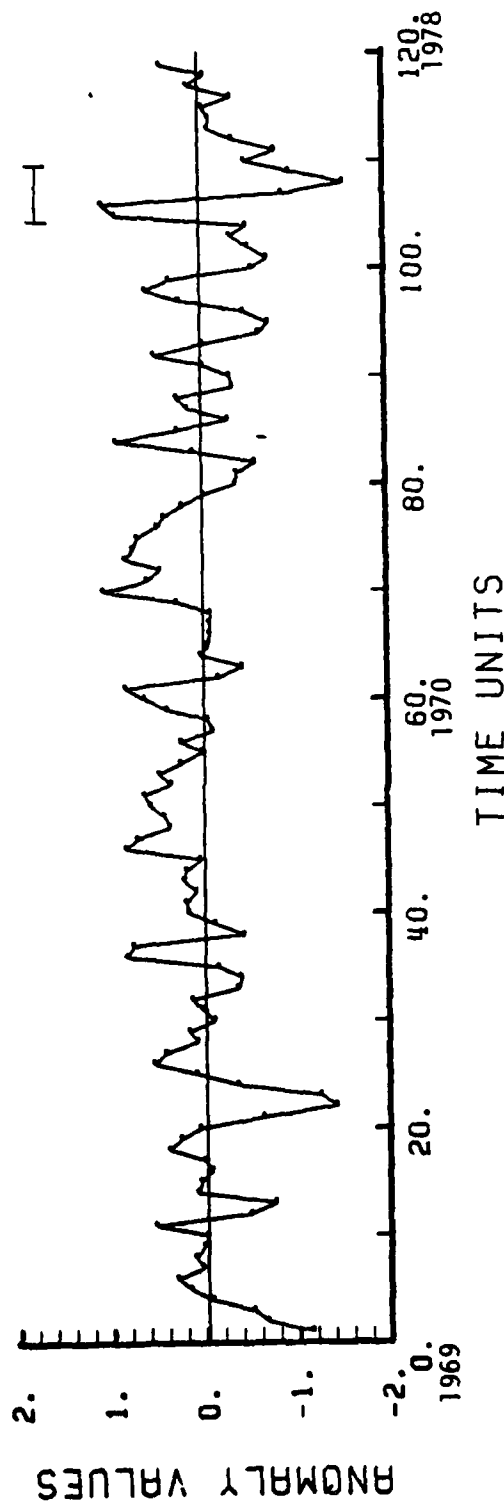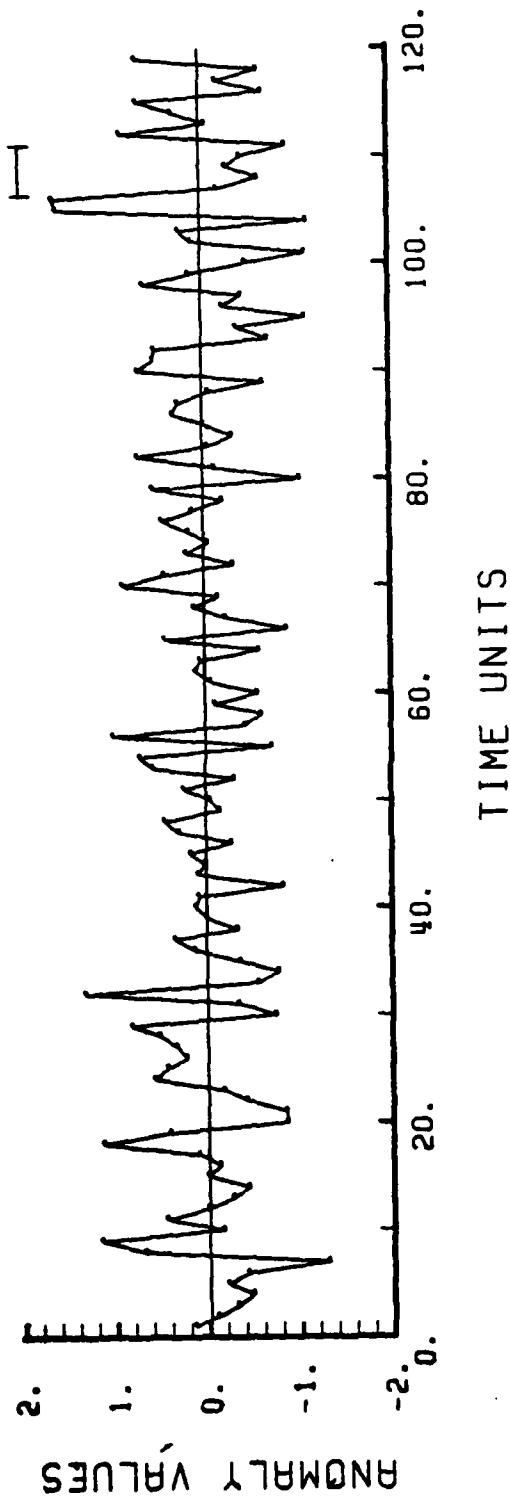
Figure 33. Average time series over Gulf of Alaska Index Area for $(U_*^3)HL$ (top, units 10^4 $(cm/sec)^3$) and $\partial/\partial t$ SST (bottom, °C month^{-1}). Time units are months where the first month is January 1969. The period chosen for synoptic analysis is shown by the horizontal bar.

70

SST

(U$_*^3$)HL
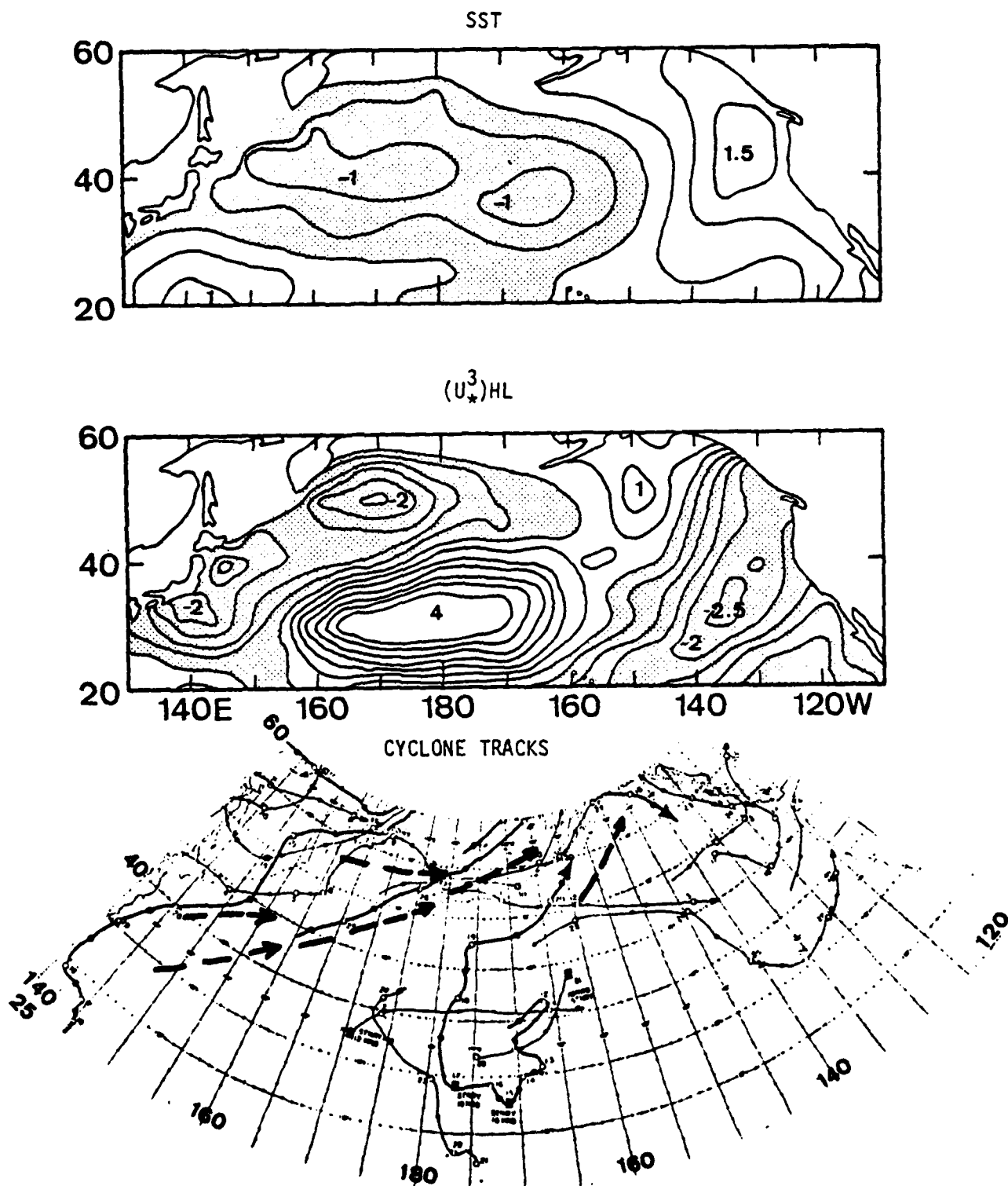
CYCLONE TRACKS

Figure 34. SST anomaly values (°C), (U$_*^3$)HL anomaly values (units 10^4 (cm/sec)^3) and cyclone tracks (Mariners Weather Log) for the month of September 1977. Contour interval is 0.5 and shaded areas denote negative values. Heavy dashes denote climatological tracks (Klein 1956).

71

SST

$(U_\star^3)$HL

CYCLONE TRACKS
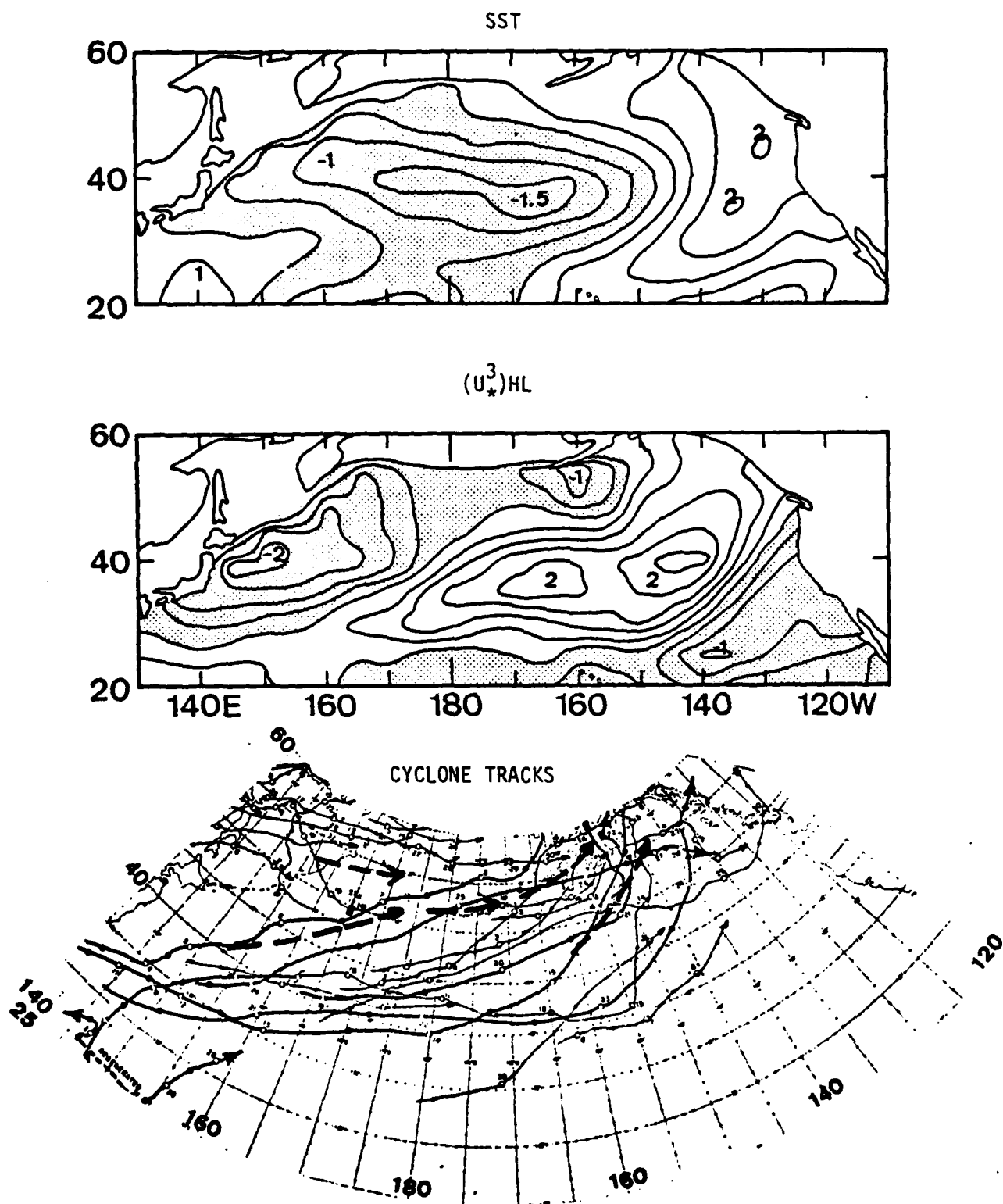
Figure 35.   Same as Fig. 34 except for October, 1977.

72

SST

(U_*^3)HL

CYCLONE TRACKS
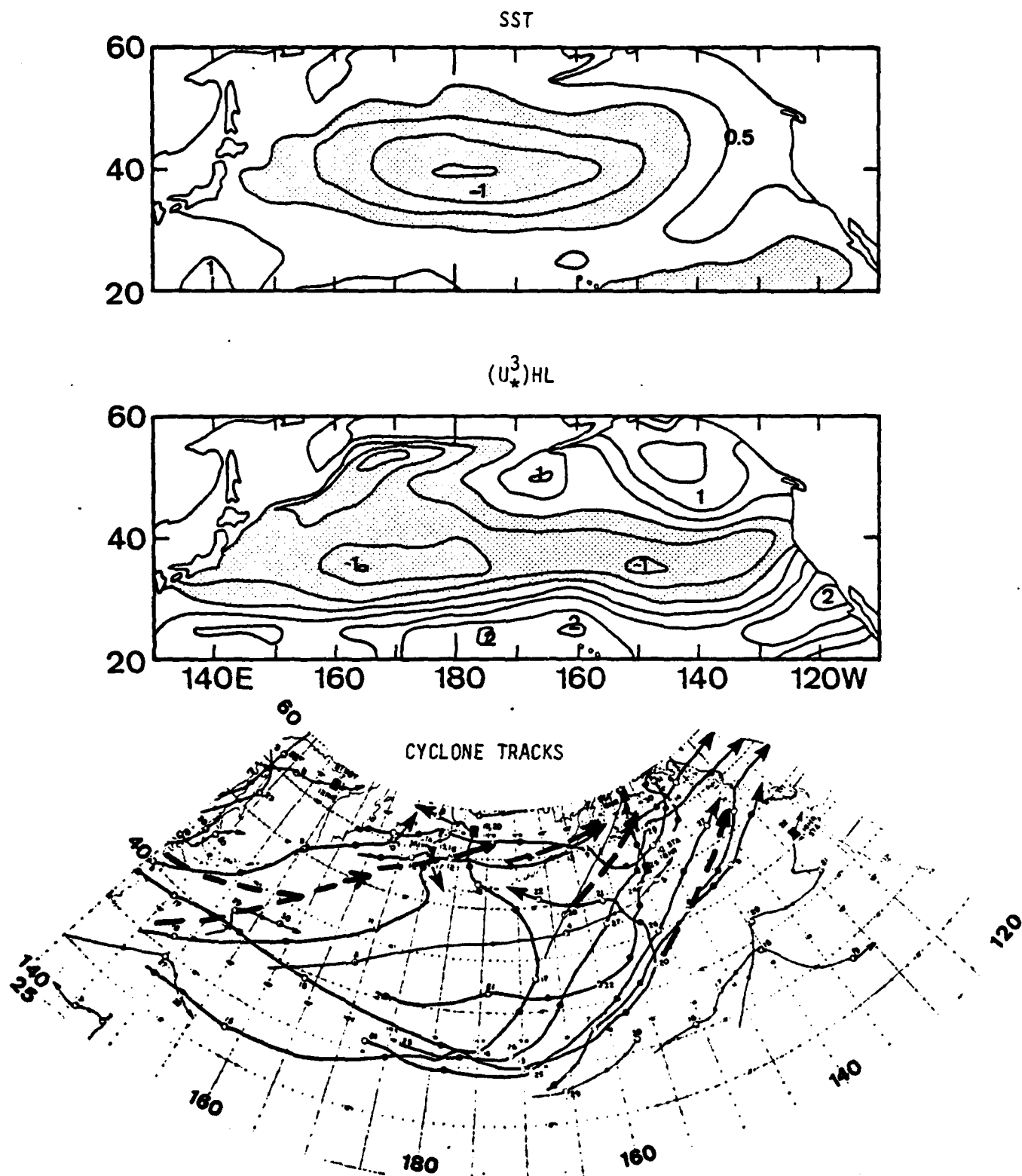
Figure 36. Same as Fig. 34 except for November, 1977.

73

The September and October (U_*^3)HL maps (middle frame in Figures 34 and 35) both show a large region of strong positive anomaly values in the Central Pacific Ocean with negative anomaly regions on either side to the East and West. This agrees quite well with the general storm track patterns as depicted in Mariners Weather Log and shown in the bottom frame of Figures 34 and 35. In addition, the September storm tracks show some isolated (and obviously anomalous) tracks in the Central Pacific Ocean which appear to be associated with a sharp trough, flanked by ridging (i.e. no storms) on either side. The October pattern, on the other hand, shows a generally southward displacement of the storm track stretching West to East across most of the Pacific. The association between November (U_*^3)HL anomaly values and the storm tracks (Figure 36) seem to agree quite well in certain areas. For example, the above normal values in the Gulf of Alaska region with negative or below normal values to the South and also in the Far Western Pacific Ocean north of Japan, seem to match the storm tracks. But there is also a region of distinct disagreement in the Central Pacific Ocean between 30° - 40° N where the storm tracks appear numerous while (U_*^3)HL is below normal.

In considering the SST response to atmospheric storminess, the absence of storm activity in the eastern part of the Pacific Ocean and the Gulf of Alaska region during the month of September appears to have brought additional warming during October. As the October storminess effect began to be felt in the Gulf, however, the trend appears to have reversed, reducing the November SST values to near normal.

Considering the qualitative nature of any estimate of cyclone frequency, it is perhaps surprising to see as much agreement between the surface wind parameter, (U_*^3)HL, and an estimate of cyclone frequency anomalies using data from the Mariners Weather Log. Given a sufficient amount of data over the ocean, it is felt that the two should tend to agree quite well. However, (U_*^3)HL should be better related to SST anomalies because of its direct physical connections via the process of turbulent vertical mixing. While it can be seen that at certain times and places (U_*^3)HL can be associated with a qualitative estimate of cyclone frequency anomalies, the comparison is very subjective.

Finally, Figure 22 (Section III) is examined to determine where the best correlations occur in relation to the mean climatological storm track. The large areas of magnitude 2 and 3 to the north in the Gulf of Alaska region and to the south in the Central Pacific region appear to indicate that the best correlations occur to the right and left of the mean track, with a weak minimum in-between. Thus the anomalous storm activity caused by North-South displacements or meanders in the storm tracks seem to show up the best in the correlations with $\partial/\partial t$ SST.

VI. CONCLUSIONS

The determination and presentation of significance levels of cross-correlations using the normalization method of Sciremammano (1979) worked very well in this study. For the atmospheric and oceanic variables considered in this study, the year-round data sets contained approximately 100 independent events (out of the 120 realizations) and the large lag standard errors were on the order of 0.1. Attempts at sub-sample record analysis reduced the realizations to approximately 10 (i.e. down by a factor of 12) and increased the σ values to approximately 0.3 to 0.4.

The application of the normalization method to the year-round data sets revealed that of the six wind parameters, the correlation of SST with $(U_*^3)H$ and with $(U_*^3)HL$ showed large areas of significant negative values in the midlatitude North Pacific Ocean when the SST was lagged by any amount from zero-to three-months. In addition, similar large areas appeared in the (zero-lag) correlations between SST and either $(U_*^3)H$ or $(U_*^3)HL$. These results appear to clearly support the hypothesis that anomalous synoptic storm activity on the time scale of a month or more is coincident with and is followed by ocean surface cooling. The most representative data set is felt to be $(U_*^3)HL$ since it considers the synoptic storm activity in the presence of the existing mean flow, and the fact it is nearly an order of magnitude larger than $(U_*^3)H$. Zero lag correlations between SST and the (U_*^3) parameters showed two areas of significant correlation in the North Pacific Ocean and support the above conclusions.

76

The (zero-lag) correlation between $\partial/\partial t$ SST and $(CURL_Z\tau)TOT$ revealed a large region of significantly positive values off the North American West Coast which may indicate an important region where positive wind stress curl anomalies are associated with monthly SST warming. This result is opposite the correlation expected from Ekman dynamics.

Examination into the possible existence of a seasonal dependence in the relationships between SST and $(U_*^3)HL$ gave results which supported the over-all hypothesis through large areas of negative correlations but did not show values which were as significant as those from the year-round record. The sub-sample record gave generally low significance levels and no statistical confidence as to the existence of a seasonal variation. The introduction of a seasonally varying mixed-layer depth did not improve the correlations over what was obtained with the constant h. Thus, the present data sets tend to suggest that there is little or no seasonal variation in the wind-SST relationships.

The investigation into the dynamics of the relationships between SST and $(U_*^3)HL$ revealed that the correlations were about the same regardless of whether $(U_*^3)HL$ was above normal or below normal, with neither being clearly dominate. The sequence September, October, November, 1977 showed good correlations between $(U_*^3)HL$ and $\partial/\partial t$ SST but attempts to see if anomalies in the maps of $(U_*^3)HL$ could be related to "apparent storm anomalies" in the Mariners Weather Log was only partially successful. At certain times and places the $(U_*^3)HL$ parameters could be associated with a qualitative estimate of cyclone frequency anomalies but the comparison was very subjective. It was found, however, that the

77

best correlations occur to the right and left of the mean climatological storm track, with a minimum in-between.

While this study has revealed large areas of statistically significant correlations between monthly anomalies of synoptic storm activity and SST, the actual raw correlations were not very large. Typical raw correlations were 0.3 with the large-lag standard error, σ, near 0.1. This generally low value of the raw correlation is an indication of the importance of other factors, both atmospheric and oceanic, which influence the SST but which were not considered in this study.

Suggestions for future research deal with an evaluation of the accuracy with which (U_*^3)HL depicts storm activity and the possible relationships between $(CURL_z\tau)$TOT and $\partial/\partial t$ SST resulting in the region of significant positive correlation observed off the North American Coast. While it is felt that (U_*^3)HL is a useful parameter in that it gives a quantitative measure of synoptic storm activity which has not been previously available, it may be desirable to check its accuracy in depicting storm activity by making this same type of synoptic comparison in a more data rich region such as the continental United States. A possible hypothesis for the significant positive correlation region off the North American Coast suggests a relationship between positive wind stress curl and below normal low level (stratus) cloudiness. The resultant increased solar radiation could possibly lead to positive SST anomalies at one- or two-months lag if this process were strong enough to dominate the cooling due to Ekman pumping. Cloud cover data for the area and time period would be required to investigate such a relationship.

78

LIST OF REFERENCES

Barnett, T. P., 1977: An Attempt to Verify Some Theories of El Nino. *J. Phys. Oceanogr.*, 7, 633-647.

Davis, R. E., 1976: Predictability of Sea Surface Temperature and Sea Level Pressure Anomalies Over the North Pacific Ocean. *J. Phys. Oceanogr.*, 6, 249-266.

Davis, R. E., 1977: Techniques for Statistical Analysis and Prediction of Geophysical Fluid Systems. *J. Geophys. Astrophys. Fluid Dyn.*, 8, 245-277.

Davis, R. E., 1978: Predictability of Sea Level Pressure Anomalies over the North Pacific Ocean. *J. Phys. Oceanogr.*, 8, 233-246.

Denman, K. L., 1973: A Time-Dependent Model of the Upper Ocean. *J. Phys. Oceanogr.*, 3, 173-184.

Elsberry, R. L. and N. Camp, 1978: Oceanic Thermal Response to Strong Atmospheric Forcing I. Characteristics of Forcing Events. *J. Phys. Oceanogr.*, 8, 206-214.

Enfield, D. B. and J. S. Allen, 1980: On the Structure and Dynamics of Monthly Mean Sea Level Anomalies Along the Pacific Coast of North and South America. *J. Phys. Oceanogr.*, 10, 557-578.

Fissel, D. B., S. Pond and M. Miyake, 1977: Computation of Surface Fluxes from Climatological and Synoptic Data. *Mon. Wea. Rev.*, 105, 26-36.

Haney, R. L., M. Risch and G. Heise, 1981: Wind Forcing Due to Synoptic Storm Activity over the North Pacific Ocean. *Atmosphere-Ocean* (in review).

Jenkins, G. M. and D. G. Watts, 1968: *Spectral Analysis and Its Applications.* Holden-Day, 525 pp.

Klein, W. H., 1956: Prevailing Tracks of Lows and Highs. *Weatherwise*, 9, 128-131.

Klein, W. H., 1956: Prevailing Tracks of Lows and Highs. *Weatherwise*, 9, 158-161.

Little, W. H., 1980: *A Statistical Study of Monthly Storminess and Sea Surface Temperature Anomalies over the North Pacific Ocean.* M. S. Thesis, Naval Postgraduate School, Monterey.

Mariners Weather Log, 1978: Smooth Log, North Pacific Weather
     September and October 1977. 3, 110-119.

Mariners Weather Log, 1978: Smooth Log, North Pacific Weather
     November and December 1977. 3, 195-204.

Preisendorfer, R. W. and T. Barnett, 1977: Significance Tests for
     Empirical Orthogonal Functions. 5th Conference on Prob. and
     Statis. in Atmos. Science. 15-18, Amer. Meteor. Soc., Boston, MA,
     169-172.

Sciremammano, F., Jr., 1979: A Suggestion for the Presentation of
     Correlations and their Significance Levels. J. Phys. Oceanogr.,
     9, 1273-1276.

Simpson, J., 1969: On Some Aspects of Sea-Air Interaction in Middle
     Latitudes. Deep Sea Res., 16, 233-261.

INITIAL DISTRIBUTION LIST

No. Copies

1. Defense Technical Information Center   2
   Cameron Station
   Alexandria, Virginia 22314

2. Library, Code 0142   2
   Naval Postgraduate School
   Monterey, California 93940

3. Chairman (Code 68Mr)   1
   Department of Oceanography
   Naval Postgraduate School
   Monterey, California 93940

4. Chairman (Code 63Rd)   1
   Department of Meteorology
   Naval Postgraduate School
   Monterey, California 93940

5. Assoc Professor R. L. Haney, Code 63Hy   1
   Department of Meteorology
   Naval Postgraduate School
   Monterey, California 93940

6. Assoc Professor C. L. Wash, Code 63Wy   1
   Department of Meteorology
   Naval Postgraduate School
   Monterey, California 93940

7. Commander   1
   Naval Oceanography Command
   NSTL Station, Mississippi 39529

8. Commanding Officer   1
   Naval Oceanographic Office
   NSTL Station
   Bay St Louis, Mississippi 39522

9. Commanding Officer   1
   Fleet Numerical Oceanography Center
   Monterey, California 93940

10. Commanding Officer   1
    Naval Ocean Research and Development Activity
    NSTL Station
    Bay St Louis, Mississippi 39522

11. Office of Naval Research (Code 480)   1
    Naval Ocean Research and Development Activity
    NSTL Station
    Bay St Louis, Mississippi 39522

12. Professor Lyle Horn   1
    Department of Meteorology
    University of Wisconsin
    1225 W. Dayton Street
    Madison, Wisconsin 53706

13. Lt. Bauke H. Houtman   2
    Rt 5 Box 228
    Escondido, California 92025

14. Lcdr. William H. Little   1
    4 Mt Tenio, Apra Heights
    FPO San Francisco, California 96630

15. Thomas L. Delworth   1
    1521 SSEC
    1225 W. Dayton Street
    Madison, Wisconsin 53706

16. Professor D. James Baker, Jr.   1
    Department of Oceanography
    University of Washington
    Seattle, Washington 98195

17. Lt. Mark E. Schultz   1
    Naval Environmental Prediction
    Research Facility
    Monterey, California 93940